FUNCTIONAL GENOMICS OF KRIT1, THE GENE MUTATED IN CEREBRAL CAVERNOUS MALFORMATION

Maxwell S. H. Lauraus

YALE UNIVERSITY

2003

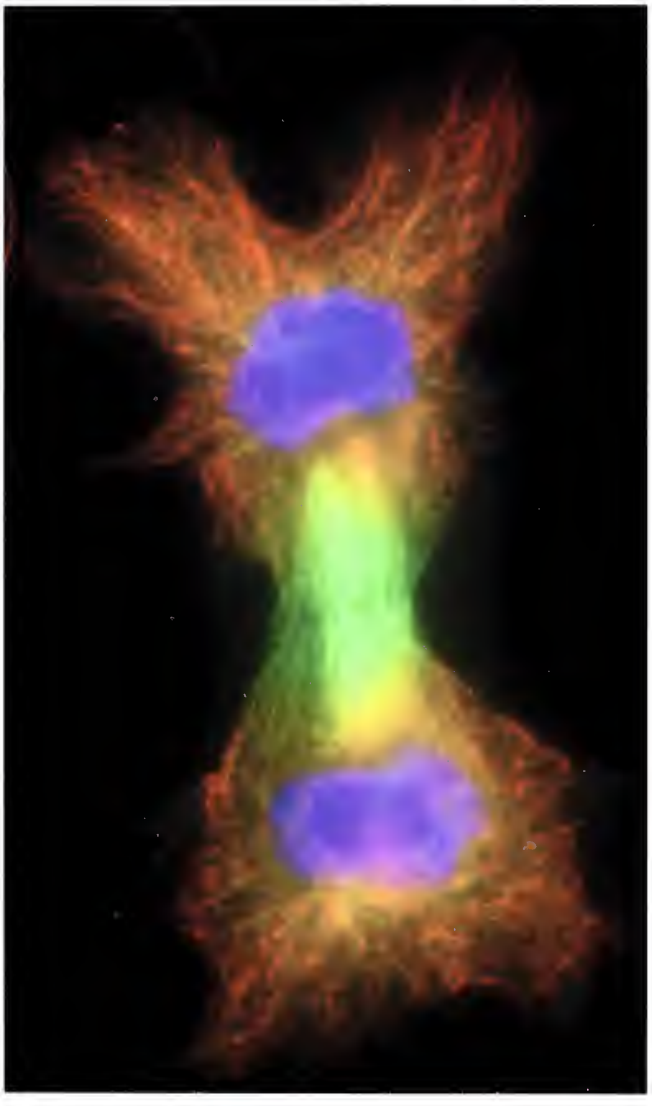

FUNCTIONAL GENOMICS OF KRIT1, THE GENE MUTATED IN CEREBRAL CAVERNOUS MALFORMATION

A Thesis Submitted to the

Yale University School of Medicine

In Partial Fulfillment of the Requirements for the

Degree of Doctor of Medicine

By

Maxwell S. H. Laurans

Thesis Advisors: Murat Gunel, M.D., and Richard P. Lifton M.D., Ph.D.

May 2003

FUNCTIONAL GENOMICS OF KRIT1, THE GENE MUTATED IN CEREBRAL CAVERNOUS MALFORMATION

Maxwell S. H. Laurans, Murat Gunel, Richard P. Lifton. Department of Neurosurgery and Department of Genetics, Yale University School of Medicine, New Haven, CT.

Mutations in *KRIT1* cause cerebral cavernous malformation, an autosomal dominant disease featuring malformation of cerebral capillaries resulting in cerebral hemorrhage, strokes and seizures. The biological functions of *KRIT1* are unknown. We have used specific anti-KRIT1 antibodies to investigate expression of this protein in endothelial cells and human tissues. KRIT1 localizes to the endothelial vasculature of diverse human tissues, and to structures important in forming the brain-blood barrier, specifically astrocyte foot processes and human cerebral endothelial cells. Within endothelial cells, by both microscopy and co-immunoprecipitation, we show that KRIT1 co-localizes with microtubules during all stages of the cell cycle. In interphase cells, KRIT1 is found along the length of microtubules. During mitosis, KRIT1 localizes in a pattern indicative of association with microtubule plus ends. These results establish that KRIT1 is a microtubule-associated protein; its location at plus ends in mitosis suggests a possible role in microtubule targeting. These findings, coupled with evidence of interaction of KRIT1 with Krev1 and ICAP1 α, suggest that KRIT1 may help determine endothelial cell shape and function in response to cell-cell and cell-matrix interactions in the CNS by guiding cytoskeletal structure. We propose that the loss of this targeting function leads to abnormal endothelial tube formation, thereby explaining the mechanism of formation of CCM lesions.

ACKNOWLEDGEMENTS

I have been unusually fortunate to have found two mentors, Murat Gunel and Richard P. Lifton, whose generous support has directed my infant medical and scientific careers. They have been the role models in whom I have found a passion for investigating medical disease and will continue to be the benchmark against which I measure myself – personally, clinically and scientifically.

I am duly indebted to all members of the Lifton and Gunel laboratories. In particular, I am grateful to Rick Wilson, as my confidant and advisor; to Michael DiLuna, who was constantly involved in this laboratory project; to Dana Shin, Carol Nelson-Williams, Faheem Niazi, Ozlem Kayisli, Umit Kayisli, and Jennifer Voorhees for technical assistance unmatched in any laboratory; to Ketu Mishra without whose help this project would have been anathema to success; and to Keith Choate, whose thoroughness, scientific dexterity, and patience I appreciated daily.

I need also thank the Howard Hughes Medical Institute and the Office of Student Research at the Yale University School of Medicine, who have been generous in their support of my growing interest in basic science research.

Finally, I thank my family – my parents, my brother, my aunts, my grandmothers, and my cousin – who, at every stage of my education, have listened without questioning, guided without directing, and always heard without my saying. I could not have asked for a more loving or understanding family to believe in my aspirations.

TABLE OF CONTENTS

FIGURES

INTRODUCTION

Cerebral Angiogenesis and Vascular Malformations of the Central Nervous System

This thesis proposes to examine the topic of cerebral angiogenesis by using the disease cerebral cavernous malformation (CCM) to develop a framework for understanding this process. Four types of vascular malformations exist in the CNS: cerebral cavernous malformations (cavernous angiomas), arteriovenous malformations, capillary telangiectasias, and venous malformations (1). When affecting the CNS, each of these malformations typically occurs in the brain, but has also been identified within the spinal cord, particularly in the case of arteriovenous malformations (2). The extent to which they might exist outside the vasculature of the central nervous system varies by specific malformation and, in the case of cavernous malformations, remains to be clarified. Unless otherwise specified, we focus the discussion here on intracranial vascular malformations.

Each type of vascular malformation has a distinct vascular architecture whose structure dictates its pathophysiology. In arteriovenous malformation (AVM), the capillary bed which normally intervenes between the arterial and venous systems does not form. The result is an unusual connection of the high pressure arterial system with the low pressure venous system, leading to venous hypertension, steal of normal arterial blood flow, and hemorrhage (3). Venous malformations are the least clinically severe form of intracranial vascular malformations, and consist of abnormally dilated veins of varied thickness and inconsistent intervening smooth muscle components (1). Rarely,

these lesions may thrombose and cause neurological deficits (4). Capillary telangiectasias, rare vascular malformations in the CNS, manifest as focal dilatations of postcapillary venules, often connecting directly with arterioles (5). These lesions more commonly exist and cause hemorrhage in mucous membranes and the gastrointestinal tract, where they are frequently recognized in their familial form - hereditary hemorrhagic telangiectasia (HHT). When cerebral, capillary telangiectasias are often associated with cerebral cavernous malformation, a disease of cerebral capillaries which fail to form tight junctions (6). In CCM, intravascular contents leak through capillary beds allowing for lesion expansion and leading to seizures, headache and neurological deficits (7).

Relatively little is understood with respect to the genetics, molecular biology, and pathogenesis of intracranial vascular malformations. Several reports indicate that arteriovenous malformations exist within multiple members of a single family, and a patient's risk of developing an AVM increases substantially if a first degree relative is diagnosed; however, genetic data does not yet explain this observation (8-14). Though not traditionally classified as vascular malformations, intracranial aneurysms also occur with increased frequency within families (15-17). These abnormally dilated blood vessels occur anywhere in the cardiovascular system, become fragile and susceptible to hemorrhage as they expand, and may lead to catastrophic hemorrhage.

Studies of families suffering the peripheral counterpart to cerebral venous malformation (VM) and capillary telangiectasia have identified genes in which germline mutations cause these vascular diseases. Activating mutations in TIE2, the receptor for angiopoietin-2, result in extracerebral venous malformations; this suggests that the TIE2

signaling pathway is important in venous development (18). Mutations in two genes, endoglin and activin receptor-like kinase 1 (ALK-1), cause hereditary hemorrhagic telangiectasia 1 (HHT1) and HHT2, respectively (19-25). Both are members of the transforming growth factor-β (TGF-β) receptor family and are expressed predominantly on the surface of endothelial cells (26). Endoglin appears to be a necessary component of angiogenesis by mouse knockout studies (27). None of these identified mutations have been implicated in cerebral vascular malformations.

Mutations of the gene *KRIT1*, the subject of this thesis, are now known to be responsible for a subset of familial cerebral cavernous malformation cases (28, 29). Though the details are largely unclear, it is apparent that each intracranial vascular malformation has a genetic component, and it is possible that some of these represent perturbations of angiogenic pathways unique to the central nervous system. It is intriguing that cavernous malformations, as well as arteriovenous malformations, are largely confined to the CNS. However, it remains unclear if the brain and spinal cord are merely more sensitive to vascular insufficiency, thereby revealing the lesion, or, alternatively, if disturbance of an aspect of angiogenesis expressed only at the vascular-CNS interface is responsible.

Clinical Presentation of Cerebral Cavernous Malformation

The clinical severity of cavernous malformations varies primarily by lesion location, and can range from an incidental finding on magnetic resonance imaging (MRI) to rare catastrophic hemorrhage. Presentation more typically occurs in the third to fifth

decades of life with symptoms of headache, intractable seizures, or focal neurological deficits due to stroke. Though female sex appears to correlate with a more clinically significant picture, especially during pregnancy, sex does not appear to predispose development of cavernous malformation lesions (30).

CCM has come to be recognized as a common clinical entity with the development of MR imaging (31). MR and autopsy studies have identified a prevalence of 0.5% for CCM in the United States population, with an estimated 20-30% of these affected individuals exhibiting symptomatic disease (7, 32-34). The T1 weighted MR appearance of cavernous malformations classically demonstrates asymmetric lesions with both hyperintense and hypointense signals (Fig 1). The appearance of blood on MR imaging is inconsistent, and may appear hyperintense or hypointense, even within hyperacute, acute, subacute and chronic categories (35). The mélange of signals which are observed in CCM lesions are thought to result from extended periods of chronic, but persistent, hemorrhage leading to a deposition of blood products in temporally diverse states of degradation. Chronic hemorrhage contributes to and/or is accompanied by relatively slow expansion of the lesion. Often, these lesions are described as "popcorn-like," owing to their budding morphology.

MR appearance of these lesions correlates well with histopathologic findings. Microscopic and ultrastructural analysis demonstrates abnormal endothelial cells which fail to form the tight junctions typical of the brain-blood barrier (36, 37) (Fig. 2a). The cells form leaky channels, or 'caverns,' through which blood is thought to hemorrhage, instead of the traditional enclosed capillary tube. In addition, lesions lack normal intervening structural support such as smooth muscle and mural elements, as well as

neural parenchyma (38). Dilated vascular spaces are visualized instead of traditional arterioles, capillaries, and venules which become histologically indistinguishable; instead, one vascular wall is shared by multiple lumen. In rare cases, cavernous malformation lesions have been identified in skin, where they demonstrate similar histopathologic features (39) (Fig. 2b). While this histopathology strongly suggests abnormal vascular development, an explanation for the focal development of CCM remains unclear.

Treatment for patients suffering cerebral cavernous malformation ranges from expectant management to anti-epileptic pharmacotherapy to surgical excision (40). The decision to treat is tailored to the individual patient and rests largely on lesion location and symptomatology. Surgical treatment is curative in patients with single lesions in the absence of an inherited or germline mutation.

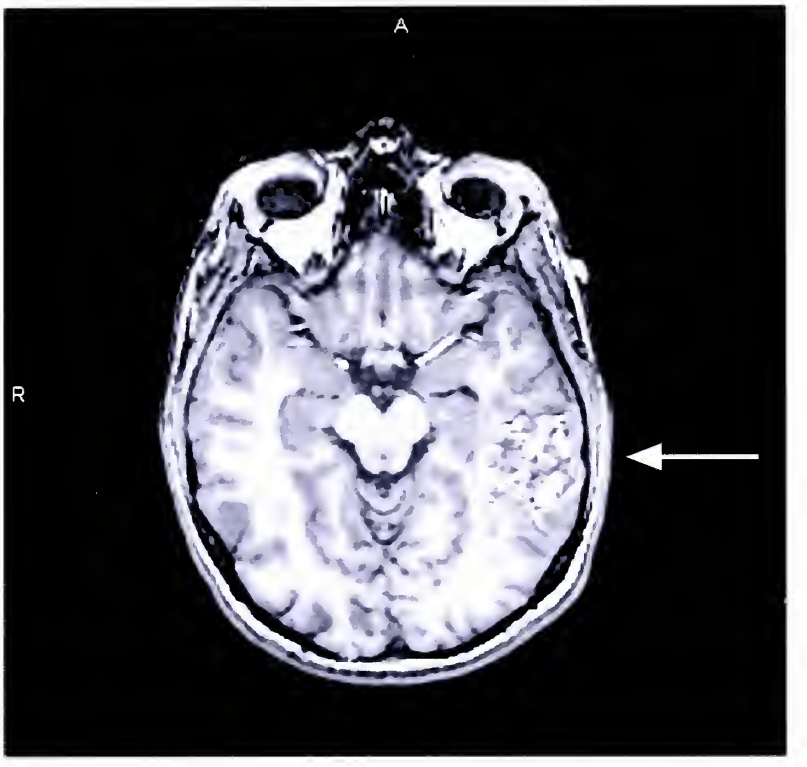

Figure 1: MRI appearance of cerebral cavernous malformation (CCM)

Axial MRI view of the brain. Characteristic cavernous malformation lesion (marked with arrow) is seen within the left temporal lobe. The heterogeneous signal within the lesion is indicative of prior hemorrhage.

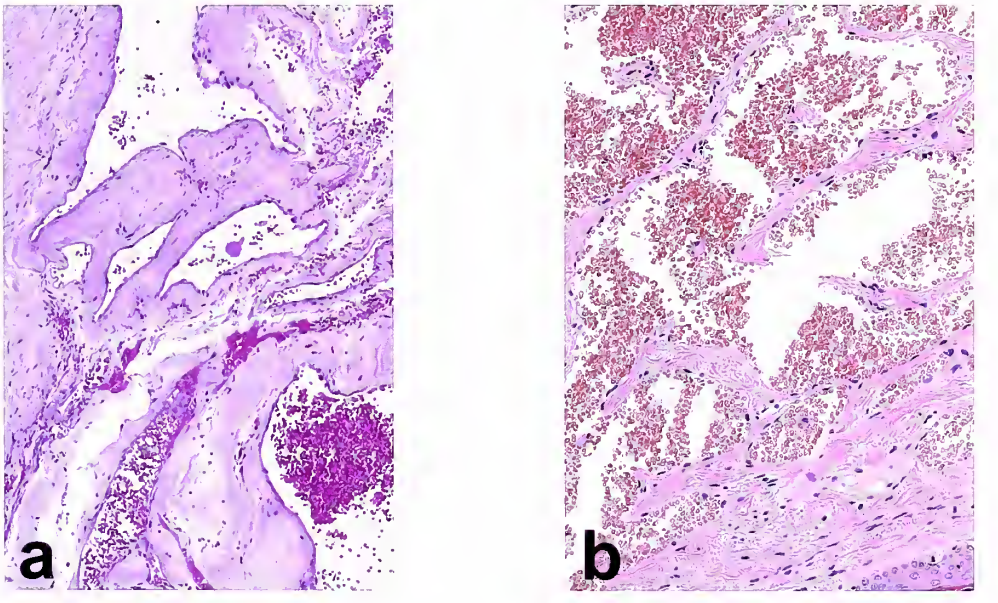

Figure 2: (a) Histology of cerebral cavernous malformation lesion (40x). (b) Histology of skin cavernous malformation lesion (40x). Both sections are stained with Hematoxalin and Eosin and demonstrate similar abnormal vasculature that defines a cavernous malformation. Arterioles, capillaries, and venules are indistinguishable, and one vascular wall is shared by multiple lumen.

The Genetics of Familial Cerebral Cavernous Malformation

Cerebral Cavernous Malformation is a disease which was long suspected to harbor both a sporadic and genetic component. As early as 1936, Michael et al. suggested that heritable factors contributed to the development of cavernous angiomas in the brain – a disease then believed to be a rare vascular disorder (41). In 1947, Kidd et al. described the occurrence of multiple cavernous malformations in a family from Iceland (42). Ten to twenty percent of Caucasian patients with CCM have a first degree relative with the disease; this proportion increases to 50% among Mexican-Americans representing a 20-100 fold increase in risk versus the general population (43), and confirming suspicions of a heritable basis for familial cavernous malformation pathogenesis. Within families that suffer from CCM, inheritance proceeds through an autosomal dominant mechanism (Fig. 3), and patients often harbor multiple cavernous malformations (Fig. 4).

Genome wide linkage analysis in the Mexican-American population initially localized one gene, *CCM1*, to 7q21 (44, 45), establishing that mutation in an unidentified gene resulted in cavernous malformation development. Further analysis of Mexican-American patients with both a positive family history and apparently sporadic disease demonstrated a founder effect among this population and a reduced penetrance for this genetic disease (46, 47). Narrowing of the linked interval to a 4 cM region on chromosome 7q (48), facilitated positional cloning experiments that proved one of the genes located in this region, *KRIT1*, as the *CCM1* gene (28, 29).

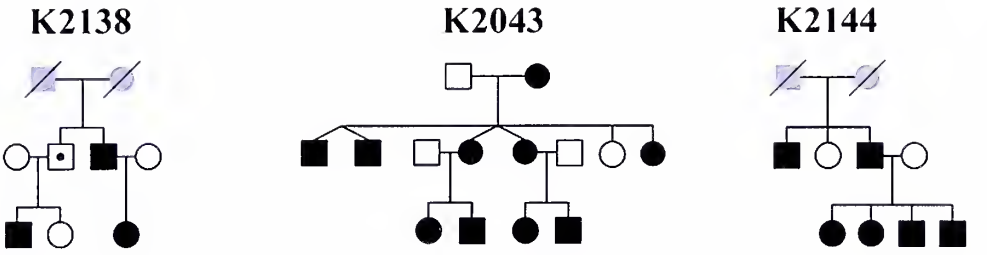

Figure 3: Representative pedigrees of families with cerebral cavernous malformation

The CCM inheritance pattern demonstrates vertical and father-son transmission, indicating autosomal dominant inheritance. Reduced penetrance is demonstrated by the presence of obligate earriers. (circle = female; square = male; grey = unknown status; white = unaffected; black = affected; dot = obligate carrier)

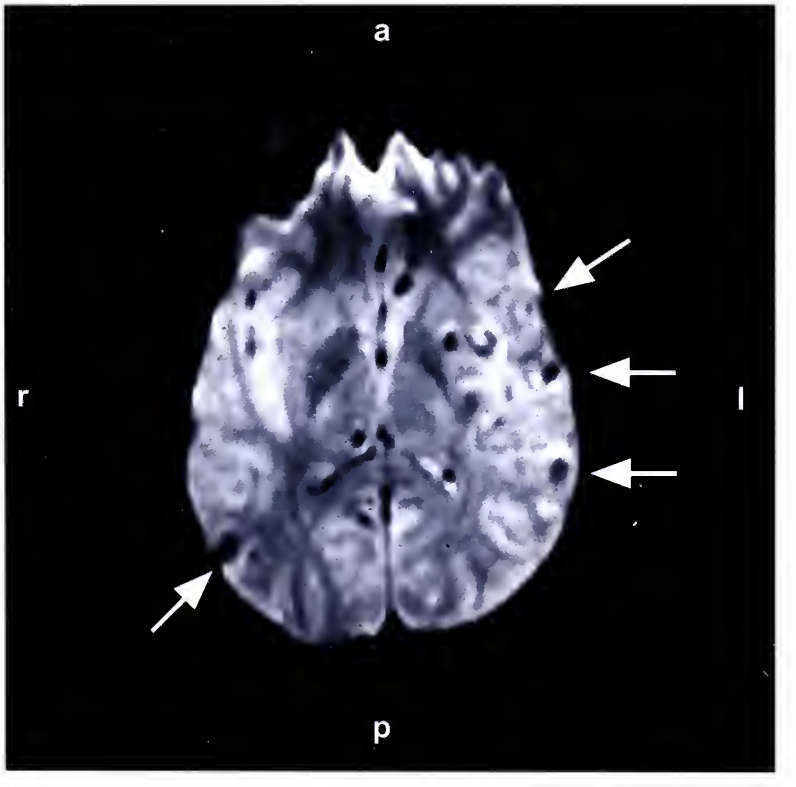

Figure 4: T1 weighted head MRI of multiple cavernous malformation lesions in a patient with a positive family history. Some lesions are indicated by arrows.

Many groups have now identified myriad mutations in *KRIT1* which are causative for cerebral cavernous malformation (28, 29, 49-56). Mutational analysis identified the founder mutation in the Mexican-American population; a single nucleotide substitution at base pair 2105 in exon 14 (2105C→T) predicted premature truncation of the KRIT1 protein (Q455X) (28, 29). The mutation has not been identified in native populations of northern Mexico or Spain (52, 57), and appears to have been the result of a germline mutation in a common ancestor subsequent to immigration to the southwestern United States.

To date, 87 mutations have been identified in patients diagnosed with cerebral cavernous malformation, and exist throughout the *KRIT1* gene (Fig. 5). With one exception, sequencing data has demonstrated nonsense, splice site, or frameshift mutations in the *KRIT1* gene, suggesting a loss of function of the resultant protein. It is unclear if this single exception, a missense mutation, is a true mutation or merely a non-functional polymorphism (53). These data are strongly suggestive of a two-hit hypothesis to explain the genetic mechanism behind cavernous malformation pathogenesis; however, only examination of CCM tissue will yield such information.

Analysis of non-Mexican-American kindreds demonstrated linkage for cerebral cavernous malformation to two additional loci: *CCM2* and *CCM3* on 7p13-15 and 3q25.2-27 respectively (47). These genes have not yet been identified.

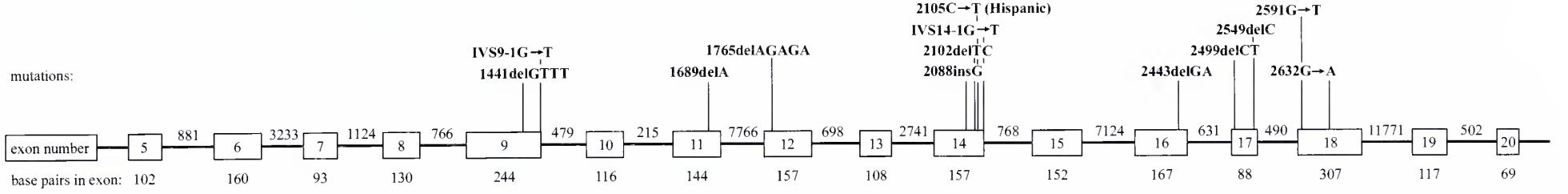

Figure 5: Graphic characterization of KRIT1 with representative mutations

Exons 5 through 20 are translated. Apparent loss of function mutations in the KRIT1 gene include splice site mutations, as well as frameshift and nonsense mutations which lead to premature truncation of the translated protein. The Hispanic-American mutation is noted.

KRIT1, the CCM1 Gene

KRIT1 was incidentally identified in a yeast-two hybrid screen using *Krev-1* (*Rap1A*) as bait (58). The gene was thus named *Krev-1/Rap1A Interaction Trapped* 1. Little was known about the function of this protein except that its carboxyl terminus was required for interaction with Krev-1 – a highly conserved 21 kDa GTPase-like protein with significant homology to the Ras family. Krev-1 has a confirmed interaction with Raf, and multiple studies have suggested that it may function as a tumor suppressor gene within the Ras signaling pathway (58, 59).

The *KRIT1* gene was initially thought to contain 12 exons which produced a 736 base pair RNA product resulting in a 63 kDa protein. Subsequent *in silico* analysis, which was later confirmed by experimental data, demonstrated that alternative splicing of this gene produced an 81 kDa protein (60, 61). Mutations throughout this larger gene have been identified in CCM families (28, 29, 49-57). Interestingly, a subsequent yeast-two hybrid study was unable to replicate the interaction between KRIT1 and Krev-1 when the larger construct is used as bait (62).

Several motifs have been identified in the KRIT1 sequence (Fig. 6). These include a Band 4.1 (FERM) domain, believed to interact with the plasma membrane, 2.5 ankyrin repeats, and an NPXY domain.

Figure 6: Suspected functional domains of the KRIT1 protein

Rationale for Investigation of the Molecular Biology of CCM: A Genetic Model for Stroke

Investigation into stroke, a disease affecting 700,000 and killing 200,000 annually, has been hampered by its multifactorial nature. Roughly 80% of strokes are ischemic, the result of thromboembolic disease. The remaining 20% of stroke cases are hemorrhagic; significant risk factors include hypertensive episodes, coagulopathic states, and cerebrovascular malformations (63).

The pathogenesis underlying stroke remains obscure. A genetic component of the disease is recognized independently of identified risk factors due to twin studies and familial aggregation of the disease (64, 65). Additionally, several Mendelian syndromes featuring stroke as a prominent component have been identified. These include cerebral autosomal dominant arteriopathy with subcortical infarcts and leukeoencephalopathy (CADASIL) and mitochondrial myopathy, encephalopathy, lactic acidosis and stroke-like episodes (MELAS) (66, 67). Identification of mutations in specific genes that lead to the stroke phenotype has fueled further investigation into the primary genetic determinants of the disease.

Cerebral cavernous malformation represents another form of Mendelian hemorrhagic stroke in which mutation of a single gene – *KRIT1*, *CCM2*, or *CCM3* – leads to an identical phenotype characterized by abnormal intracranial vascular development and hemorrhagic stroke. A specifie role for KRIT1 in the development or maintenance of the CNS vasculature remains unclear; however, it is likely that both the *CCM2* and *CCM3* gene products contribute to this unrecognized system in series or in parallel, given

that patients who link to any of these three loci develop lesions which are phenotypically indistinguishable. Hence, cerebral cavernous malformation functions as an unusual, naturally occurring, model of hemorrhagic stroke; by studying the exception, we seek to elucidate the rule.

Understanding the normal function of KRIT will provide clues to a mechanism which explains CCM pathogenesis and the predominant existence of lesions within the intracranial vasculature. In rare cases, cavernous malformation lesions in patients with known *KRIT1* mutations have been identified in the skin and retina, though they do not appear to exist independently from cerebral lesions (49, 50, 68). A role for KRIT1 in intracranial capillaries is poorly understood and its expression pattern and potential function in extracerebral human tissue remains completely uncharacterized. The histopathology of cavernous malformation lesions suggests that KRIT1 may be important in dictating endothelial cell morphology and in intercellular communication; mutation of this protein appears to perturb capillary development in a subset of the endothelial cell population. We hypothesize KRIT1 is important in endothelial cell morphogenesis and that it specifically affects cerebral capillary development, and cerebral angiogenesis.

METHODS

(Antibody characterization, Western blotting, immunofluorescence microscopy, and RT-PCR were performed with the assistance of Dana Shin and Michael DiLuna. Immunoprecipitation and immunocytochemistry visualized by confocal microscopy were performed solely by the author. Immunohistochemistry visualized by light microscopy was performed with the assistance of Ozlem Kayisli.)

In vitro cell cultures. Bovine Aortic Endothelial Cells (BAE cells) (supplier ATTC, Rockville, MD) at early passages (<6) were cultured in high glucose Dulbecco's modified Eagle's Medium (DMEM) (Gibco BRL, Carlsbad, CA) with 10% Fetal Bovine Serum, 100 mM HEPES, 10 mM sodium pyruvate, 100 U ml^{-1} penicillin G, 100 mg mL^{-1} streptomycin, and 0.25 mg ml^{-1} amphotericin B. COS7 cells were grown in low glucose DMEM with 10% fetal bovine serum and 100 U ml^{-1} penicillin G, 100 mg mL^{-1} streptomycin, and 0.25 mg ml^{-1} amphotericin B. Cells harvested for Western blot and RT-PCR analysis were seeded on 100 mm dishes at a concentration of 1 X 10^7 cells/dish and grown to confluence.

For treatment with the microtubule-depolymerizing drug nocodazole, BAE cells were plated on glass slides and cultured. The cells were then treated for 24 hours with 10 μM of nocodazole and fixed prior to immunocytochemistry. Control cells were cultured without nocodazole and fixed and assayed at the same time points. For actin depolymerization, BAE cells were incubated with cytochalasin D (Sigma, Saint Louis, MO) for 30 minutes prior to fixation.

RT-PCR of Bovine Aortic Endothelial cell mRNA. Total cellular RNA was extracted from cells grown in tissue culture dishes using Trizol (Gibco BRL, Carlsbad, CA) and cDNA was produced via reverse transcription. PCR was performed on cDNA using primers specific for *KRIT1* (sense – 5' TACATATGGGCTATAGTGCAC and antisense – 5' TATCAGCTTAGCATCAGGAGCTG), yielding a 1040 bp fragment. Primers for GADPH were used to control for RT-PCR efficiency and cDNA synthesis (sense – 5' CCTCTGGAAAGCTGTGGCGT and antisense – 5' TTGGAGGCCATGTAGGCCAT) yielding a 430 bp fragment.

KRIT1 antibodies. Synthetic peptides corresponding to the following hydrophilic segments of KRIT1 were produced: Peptide 1 (KRIT1 259-275), DYSKIQIPKQEKWQRS, Peptide 2 (KRIT1 473-490), QLEPYHKPLQHVRDWPE, Peptide 3 (KRIT1 724-736, C-terminus), *GGG*KLNGQLMATERNS. After conjugation to KLH, peptides were injected into rabbits and boosted twice; resulting antipeptide antibodies were affinity purified using the immunizing peptide (Zymed Laboratories, San Francisco, CA). Antibody specificity was tested by Western blotting.

Characterization of KRIT1 antibodies by Western blot. COS7 cells expressing His-tagged KRIT1 (expected size 62 kDa) from a pcDNA4/HisMax/Xpress plasmid (Invitrogen, Carlsbad, CA) were lysed and the products fractionated by SDS-PAGE. Antibodies were applied to resulting membranes and visualized by chemiluminescence (NEN, Boston, MA) (69).

For protein extraction from endothelial cells, cells were scraped directly into boiling sample buffer (100 mM Tris pH 6.8, 200 mM DTT, 4% SDS, .2% Bromophenol Blue, and 20% Glycerol) prior to loading on gels. For SDS-PAGE, protein samples were

fractionated by electrophoresis on a 10% acrylamide gel and transferred to membrane. Blots were blocked in 10% non-fat dried milk in PBS with 0.05% Tween-20. Blots were incubated with primary antibody and staining was detected by incubation with HRP donkey-anti-rabbit antibody followed by chemiluminescence. For peptide competition assays, primary antibody was competed by a 4-fold molar excess of the immunizing peptide prior to incubation.

Tissue collection and preparation. Human adult tissues were obtained from the Department of Pathology, Yale University School of Medicine (protocol # 7680). Informed consent was obtained and protocols were approved by the Human Investigation Committee. Each tissue was divided into three sections for analysis by RT-PCR, Western blot, and immunohistochemistry. Protein extraction was carried out immediately following tissue collection using T-PER tissue protein extraction reagent (Pierce, Rockford, IL) supplemented with a protease inhibitor cocktail, as was RNA extraction using Trizol reagent (Gibco BRL, Carlsbad, CA); tissue to be used for immunohistochemical analysis was fixed overnight in 4% paraformaldehyde, embedded in paraffin, cut to a thickness of 5-7 μm, and mounted on gelatin-coated slides.

Semi-quantitatvie analysis of KRIT1 transcription by PCR. A cDNA library (Clontech, Palo Alto, CA) was used to assess KRIT1 transcription in human fetal tissues. PCR was performed using primers specific for *KRIT1* (sense – 5' ACTGGGAAGAAGCTGCAAAA and antisense – 5' CTGTGAAAAATGCTGCTCCA), yielding a 717 base pair fragment. Primers for actin were used to control for RT-PCR efficiency and cDNA synthesis (sense – 5' TTGCTGATCCACATCTGCTG and antisense – 5' GACAGGATGCAGAAGGAGAT) yielding a 120 base pair fragment.

Resulting signal was quantified by a digital imaging and analysis system (AlphaEase, Alpha Innoteh Corporation San Leandro Ca) where the intensity of each KRIT1 band was normalized to its corresponding actin band such that semi-quantitative comparison could be made between samples.

Semi-quantitative analysis of KRIT1 expression by Western blot. Protein concentration was determined by a detergent compatible protein assay (Pierce). For SDS-PAGE, 20 μg protein samples were fractionated by electrophoresis on a 7.5% Tris-HCl acrylamide gel and transferred to nitrocellulose membrane. Blots were blocked in 5% non-fat dried milk in PBS with 0.05% Tween-20, incubated with primary antibody followed by HRP donkey anti-rabbit secondary antibody, and visualized by chemiluminescence (69), or HRP mouse anti-human GADPH antibody (Santa Cruz Biotecnology, Santa Cruz, CA). Membranes were subsequently stripped and reprobed with HRP mouse-anti-human GADPH antibody to confirm that equal amounts of protein was loaded. Bands visualized on Western blot were quantified using a laser densitometer (AlphaEase, Alpha Innoteh Corporation San Leandro Ca), and KRIT1 signal was normalized to signal generated by GADPH.

Immunohistochemistry. Tissue sections were de-paraffinized and re-hydrated in an alcohol gradient prior to analysis by a standard streptavidin-biotin technique. Endogenous peroxidase activity was blocked by incubation in 3% H_2O_2 (0.6 ml of H2O2 and 2.7ml of methanol and 2.7 ml of d H2O). Slides were blocked with 5% normal goat serum, incubated overnight with human polyclonal rabbit anti-KRIT1 antibody at 4 °C, and incubated for 30 min at 25 °C with secondary biotinylated goat anti-rabbit IgG (Vector Laboratories, Inc., Burlingame, CA). Slides were incubated with the

streptavidin-peroxidase complex using the Vectastain ABC Elite kit (Vector Laboratories). Chromogenic reactions were completed with 3-amino 9-ethyl carbazole (AEC) to yield a positive red stain, or 3, 3'-diaminobenzidine (DAB) to yield a positive brown stain (Vector Laboratories, Inc.). Slides were counterstained with haematoxylin prior to mounting and visualization by light microscopy. All immunostaining with anti-KRIT1 antibody was competed with a two-fold molar excess of the immunizing peptide. Subsequent incubation with secondary antibody and evaluation as above yielded no signal.

Intensity of staining by KRIT1 antibodies was semi-quantitatively evaluated. Two investigators, acting independently, scored five 40x high power fields (HPFs) for percentage of positively stained cells within the following categories: – (no staining) 1+ (weak but detectable), 2+ (moderate or distinct), 3+ (intense). For each cell type or tissue section, an HSCORE value was derived according to the following formula:

$$HSCORE = P_i\,(i+1)$$

where i represents the intensity scores and P_i is the corresponding percentage of the cells.

Immunoprecipitation. For immunoprecipitation, adherent Bovine Aortic Endothelial Cells (BAE cells) were grown to confluency and lysed in ice-cold cytoskeletal lysis buffer (0.5% NP-40, 10 mM Pipes pH 6.8, 50 mM NaCl, 300 mM sucrose, 3 mM $MgCl_2$) with protease inhibitors (4-(2-aminoethyl)benzenesulfonyl fluoride (AEBSF), pepstatinA, E-64, bestatin, leupeptin, and aprotinin) (Sigma, Saint Louis, MO). The lysate was precleared with Protein G Plus-Agarose (Oncogene, La Jolla, CA), after which β-tubulin antibody (developed by Michael Klymkowsky, obtained from the Developmental Studies Hybridoma Bank developed under the auspices of the NICHD and maintained by The

University of Iowa, Department of Biological Sciences, Iowa City, IA 52242) or KRIT1 antibody, separately coupled to Protein G Plus Agarose, was used for immunoprecipitation. After overnight incubation at 4 °C, beads were collected by centrifugation, washed with lysis buffer, boiled and fractionated by SDS-PAGE gel electrophoresis and analyzed by Western blotting as described above.

Immunocytochemistry. Cells were split onto microscope slides and grown for 24 hours. The slides were washed with PBS, fixed with 3% paraformaldehyde, and permeabilized in 0.2% Triton-x100 in PBS. The sections were blocked with 10% normal donkey serum (NDS) and 1% BSA in PBS. They were incubated with primary followed by secondary antibody, stained with DAPI and mounted. β- and α-tubulin primary antibodies were purchased from Sigma. For actin staining, cells were incubated with 1 μM Phalloidin (Sigma, Saint Louis, MO) conjugated to rhodamine. For cold induced fracture of microtubules, BAE cells were incubated in ice cold PBS for varying amounts of time and allowed to recover at 37 °C, followed by immunocytochemistry.

RESULTS

Antibody characterization

Antibodies to KRIT1 peptides were produced and affinity purified. Resulting antibodies were tested for specificity by Western blotting and immunohistochemistry. Antibodies directed against the 13 amino acid peptide at the C-terminus of the protein specifically stained a peptide of the expected size in extracts of COS7 cells transfected with a his-tagged KRIT1 construct (Fig. 7a). This staining is competed with the immunizing peptide (Fig. 7b) demonstrating its specificity.

KRIT1 is expressed in endothelial cell lines

The antibody also identified a product of the expected size for endogenous KRIT1 in untransfected bovine aortic endothelial (BAE) cells (Fig. 8a). RT-PCR analysis confirmed the presence of *KRIT1* mRNA (Fig. 8b) in BAE cells, and the sequence of this product identified it as the *KRIT1* ortholog (86% nucleotide and 85% amino acid sequence identity to human KRIT1).

Relative expression of KRIT1 in human tissue

Expression of KRIT1 in human tissue was evaluated by examining extracted protein on Western blot and probing with KRIT1. KRIT1 is expressed strongly in human kidney, liver, and lung, moderately in pancreas and spleen, and weakly in brain (Fig. 9). Expression in fetal tissue was examined by using a human fetal cDNA library, and demonstrated a similar pattern of distribution (Fig. 10).

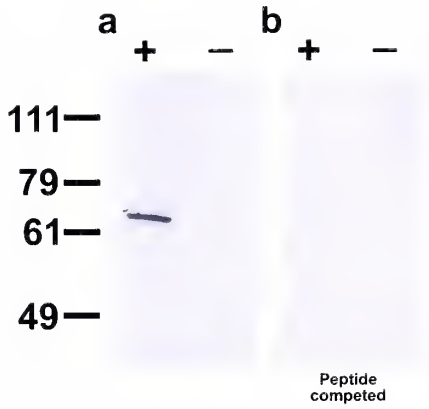

Figure 7: Characterization of specific anti-KRIT1 antibodies

Anti-KRIT1 antibodies were used to stain Western blots of extracts of COS7 cells. These cells, which do not express endogenous KRIT1, were transfected either with plasmid expressing his-tagged KRIT1 (+) or an empty vector (-) as described in methods. (a) Staining detected a protein of size expected for the fusion protein in cells transfected with KRIT1. (b) Peptide competition eliminates staining, demonstrating the specificity of this antibody for the KRIT1 protein.

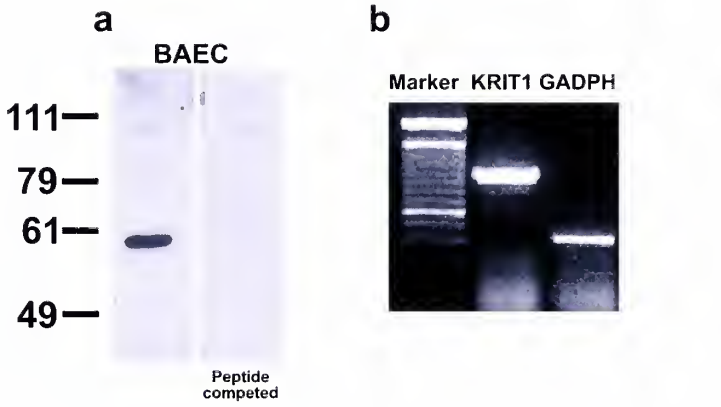

Figure 8: (a) Western blot of native BAECs using anti-KRIT1. A 58 kDa band is detected when protein isolated from BAEC cultures is probed with anti-KRIT1 antibodies; this band is competed by the immunizing peptide. (b) RT-PCR reveals KRIT1 mRNA expression in BAECs. The sequence of the product reveals an encoded protein of 85% identity with human KRIT1.

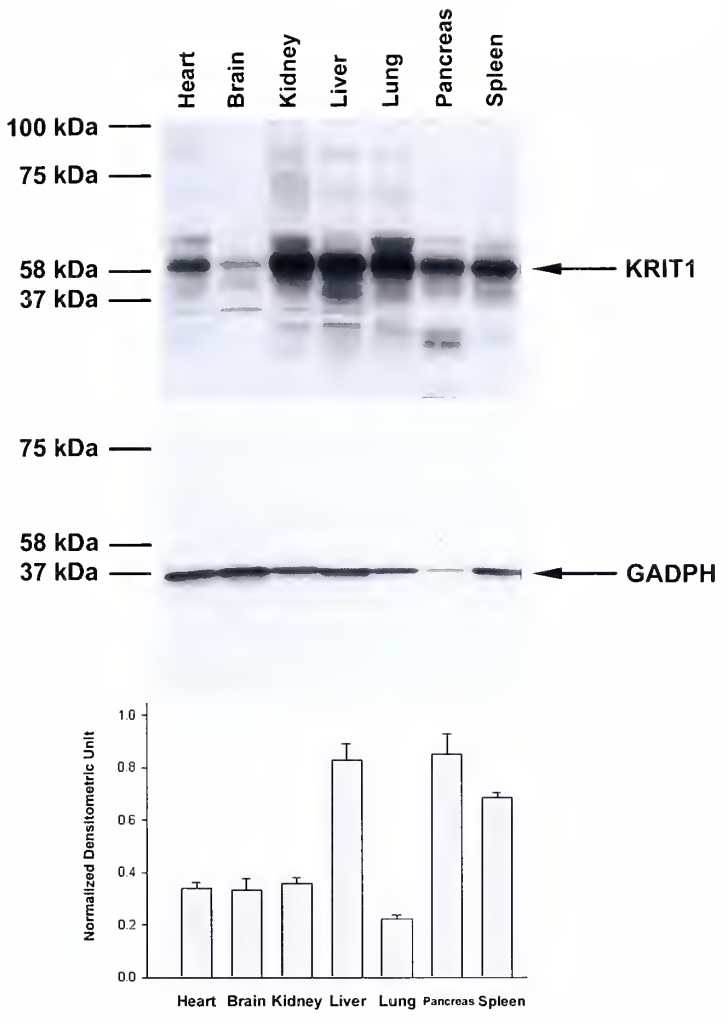

Figure 9: KRIT1 is expresed in diverse human tissues

Expression of KRIT1 protein in human tissue was evaluated by Western blot probed by antibodies specific for KRIT1. Equal amounts of protein were loaded in each lane, and blots were probed for KRIT1, stripped and then probed for GADPH. Band signal was quantified, and normalized to housekeeping protein GADPH such that meaningful comparisons could be made between tissue types. The protein is expressed strongly in kidney, liver, and lung, moderately in pancreas and spleen, and weakly in brain.

Figure 10: Relative expression of KRIT1 in human fetus

Quantitative RT-PCR was performed using a cDNA library to assess for KRIT1 transcription level. RNA was quantified subsequent to reverse transcription, and resulting signal intensity was normalized to that of actin in each respective sample. KRIT1 is most strongly expressed in liver, and moderately expressed in lung, kidney, spleen and thymus.

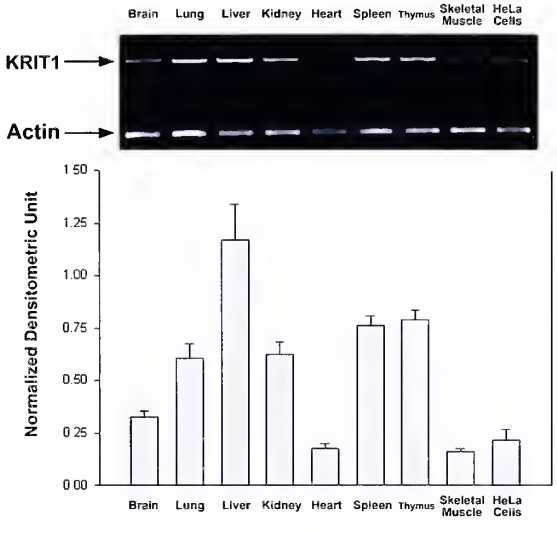

Immunolocalization of KRIT1

Localization of KRIT1 within adult human tissue was determined by immunohistochemical staining of paraffin embedded tissue which was visualized by light microscopy after streptavidin-biotin exposure.

KRIT1 stains endothelial cell cytoplasm in human brain tissue, the cell in which we hypothesized the disease phenotype would primarily manifest (Fig. 11a). Semi-quantitative analysis of staining in the cerebrovasculature indicates that endothelial cells of capillary beds and arterioles stain more intensely than venous counterparts (Fig. 11b). In larger, more complex vascular structures, the tunica intima stains most intensely, followed by the foot processes of astrocytes which abut the tunica adventitia. The smooth muscle of the tunica media does not react with antibodies directed to KRIT1.

In the cortex of brain parenchyma, anti-KRIT1 antibodies positively stain the cytoplasm of select neuronal cell bodies in cortex layers 1-6, with cortex layer 5, the internal pyramidal layer, exhibiting the most intense staining (Figs. 12 & 13). In particular, the cytoplasm of select pyramidal cells of both the internal and external pyramidal layers (cortex layers 3 and 5) react with antibodies directed to KRIT1. Other cells in the granular layers do not stain for KRIT1.

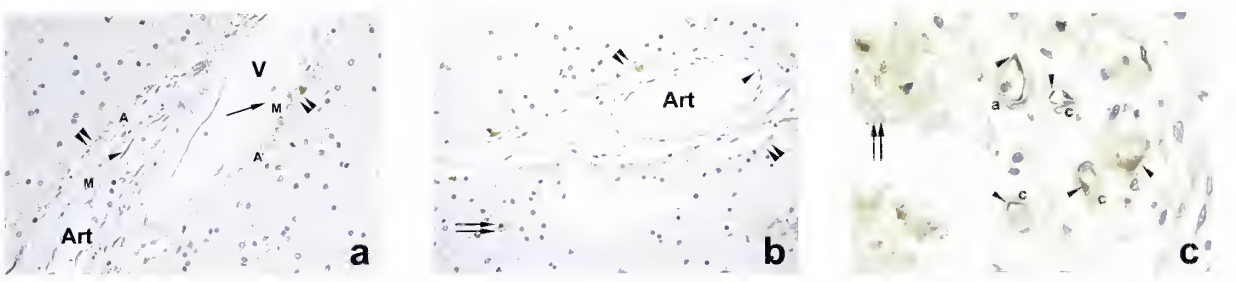

Figure 11a: KRIT1 expression in human cerebrovasculature

Specific antibodies directed to KRIT1 were incubated in slides of paraffin embedded human adult brain. The resulting streptavidin-biotin reaction reveals a brown signal to indicate a positive stain. (a) Endothelial cells of the cerebral vein (V) stain weakly for KRIT1 (arrow), while those of the corresponding artery (Art) stain more strongly (arrowhead). Foot processes of astrocytes abutting the tunica adventitia (A) stain positively for KRIT1 (double arrowhead). (b) Endothelial cells of the artery stain positively for KRIT1 along with astrocytic foot processes. The cytoplasm of additional astrocytes also stain positively for KRIT1 (double arrow). (c) Endothelial cells of cerebral capillaries (c) react with antibodies directed to KRIT1, as do endothelial cells of arterioles (a).

(V = vein; Art = artery; A = tuniea adventitia; M = tunica media; I = tunica intima; arrow = weakly/absent staining endothelial cells; arrowhead = intensely staining endothelial cells; double arrowhead = astrocytic foot processes; double arrow = astrocyte; a = arteriole; c = capillary)

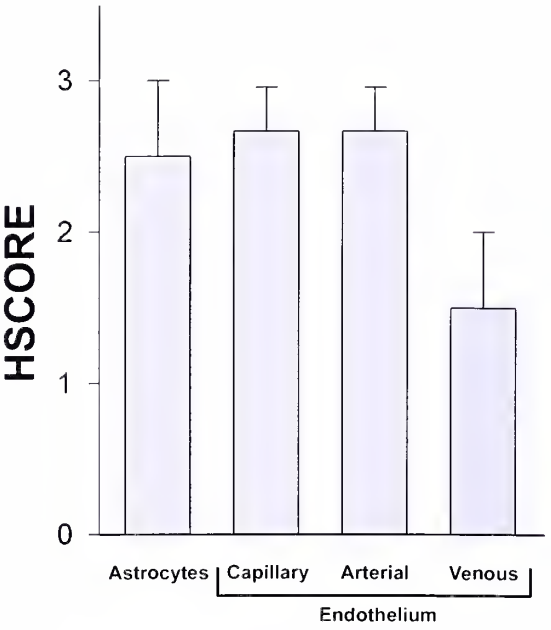

Figure 11b: Semi-quantitative analysis of KRIT1 expression by cerebral cell type

Degree of staining for KRIT1 protein was assessed semi-quantitatively and categorized by cell type. Cells of capillary bed endothelium and arterioles stain more strongly than venous counterparts.

Figure 12: Immunolocalization of KRIT1 in the cerebral cortex

Paraffin embedded sections of human cerebral cortex were stained with anti-KRIT1 antibodies (brown). KRIT1 protein is present in pyramidal neurons which are most most commonly located in cortex layers 3 and 5, the internal and external pyramidal layers. (arrow = positively staining cell)

Figure 13: KRIT1 stains pyramidal cells in the cerebral cortex

In this section from the internal pyramidal layer, cortex layer 5, KRIT1 antibodies intensely stain pyramidal neurons (red). (Arrowhead = positively staining cell)

KRIT1 is present in vascular structures of varied organs in the human body. In each organ, KRIT1 is primarily expressed by small vessels including capillary beds and arterioles, and rarely expressed by larger vascular structures. KRIT1 stains the endothelium most strikingly in organs with an extensive vascular supply such as liver and spleen (Fig. 14). In the heart and in skeletal muscle, markedly intense staining for KRIT1 is observed in arteries, while expression in veins is absent (Fig. 14a & 14b). In skin, endothelial cells of arterioles and capillaries stain for KRIT1 in the dermis; this is most striking among the small vessels which comprise the sub-papillary plexus. Epithelial cells of sweat glands, the ducts of these glands and hair follicles also express KRIT1. The epidermis, which lacks significant vascular supply, does not express KRIT1 except in the stratum basale. This cuboidal layer of cells lies at the junction between the dermis and epidermis, is joined to the basement membrane by hemi-desmosomes, and stains weakly for KRIT1 (Fig 14c). In the liver, KRIT1 staining is absent in the portal vein but present in arteriolar branches of the hepatic artery that run through the portal tract; the protein is not expressed by the fenestrated capillaries of hepatic sinusoids in the liver parenchyma (Fig. 14d). Numerous small branches of the inferior thyroid and internal thoracic arteries enter the thymus at the interlobular septa that is continuous with the collagenous capsule surrounding the lymphoid organ. KRIT1 distinctly stains the endothelial cells of these branches, but not their corresponding venous counterparts (Fig. 14e).

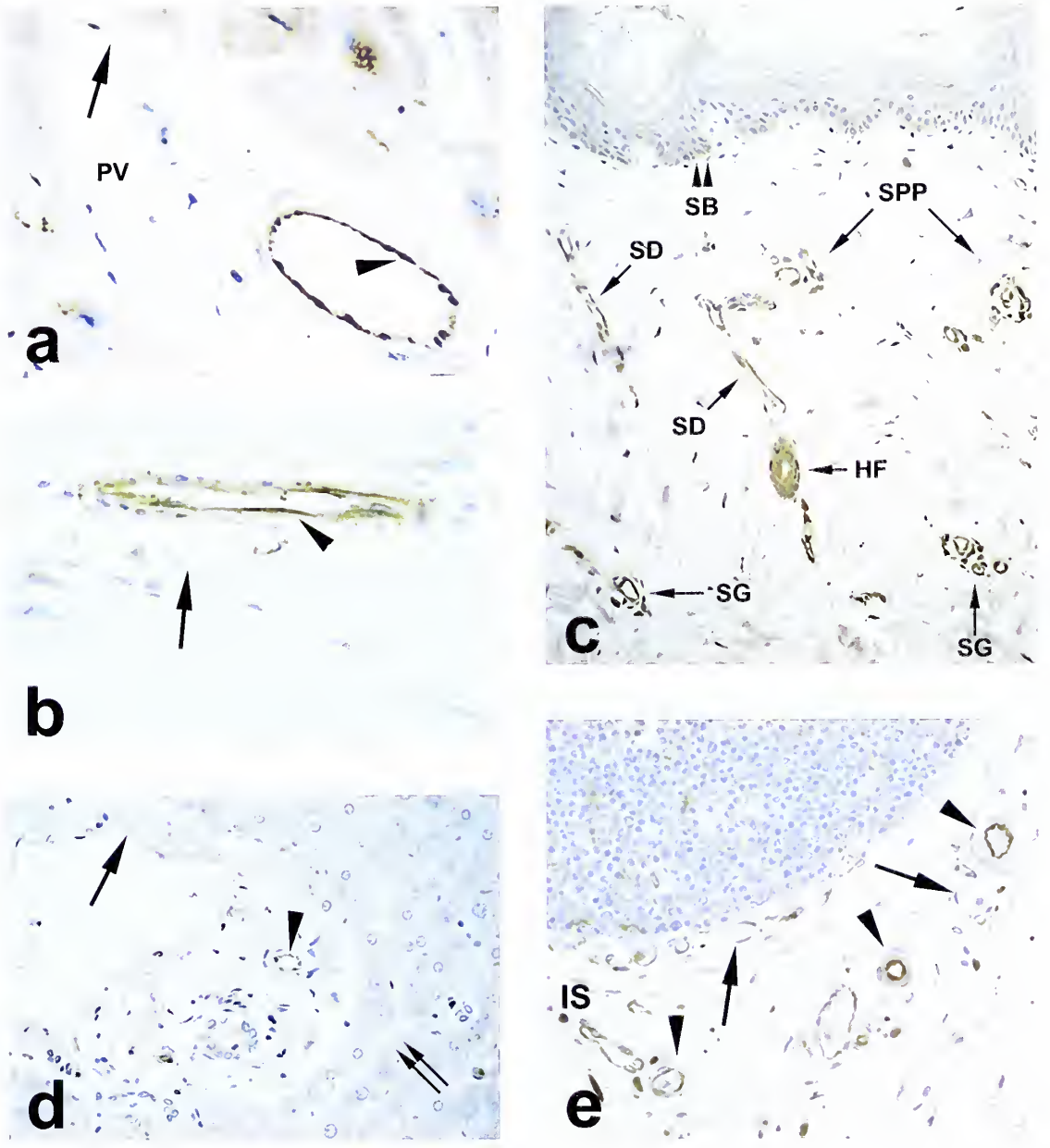

Figure 14: KRIT1 localization in vascular endothelium of heart, skeletal muscle, skin, liver, and thymus

Paraffin embedded sections of human tissue were stained with anti-KRIT1 antibody (brown). (a) In heart arterial endothelium, antibodies to KRIT1 yield an intense positive signal (arrowhead) while the corresponding vein lacks signal altogether (arrow). (b) Arterial endothelium of skeletal muscle stains positively for KRIT1 while the corresponding vein does not react with antibodies to KRIT1. (c) Endothelial cells of arterioles and capillaries in the sub-papillary plexus of the dermis (SPP) stain positively for KRIT1, as do epithelial cells of sweat glands (SG), sweat ducts (SD), and hair follicles (HF). Weak staining is observed in the stratum basale (SB, double arrowhead). (d) The thin endothelial cells of the portal vein (PV) fail to react with anti-KRIT1 antibodies while arteriolar branches of the hepatic artery stain for the protein (arrowhead). (e) Branches of the inferior thyroid and internal thoracic artery stain positively for KRIT1 where they enter the thymus at the interlobular septa (IS) while corresponding venules do not. (arrow = endothelial cell without staining for KRIT1; arrowhead = endothelial cell positively staining for KRIT1; SB, double arrowhead = stratum basale; SPP = sub-papillary plexus; SG = sweat gland; SD = sweat duct; HF = hair follicle; double arrow = hepatic sinusoid; PV = portal vein; IS = interlobular septa)

This data establishes the presence of KRIT1 in human endothelial cells, but fails to characterize the specific function of this protein. We hypothesize that subcellular KRIT1 influences endothelial cell morphogenesis and that its mutation prohibits normal microvascular development.

KRIT1 is associated with microtubules

We localized KRIT1 in BAE cells by immunocytochemistry. During interphase, we observed that KRIT1 localized to the cytoplasm with a pattern suggesting association with a component of the cytoskeleton (Fig. 15). To further characterize this pattern, we used double and triple staining with antibodies directed against KRIT1 and either actin, or tubulin (Fig. 16). KRIT1 showed co-localization with tubulin, but not with actin. Confocal microscopy confirmed the same pattern of co-localization with KRIT1 showing a granular staining pattern along the length of microtubules (Fig. 17).

This association of KRIT1 with tubulin was further explored by treatment of BAE cell cultures with nocodazole, which depolymerizes microtubules (70). Following nocodazole treatment, both tubulin and KRIT1 staining showed characteristic cytoplasmic "clumps" instead of the typical spindle pattern (Fig. 18). Disruption of microtubules with cold also confirmed KRIT1's association with microtubules (Fig. 19). The continued co-localization with tubulin demonstrates the association of KRIT1 and tubulin in both polymerized and depolymerized states (Figs. 18 & 19) suggesting that KRIT1 is a microtubule-associated protein.

Actin depolymerization with cytochalasin D did not have any effect on KRIT1 staining or its association with microtubules (data not shown).

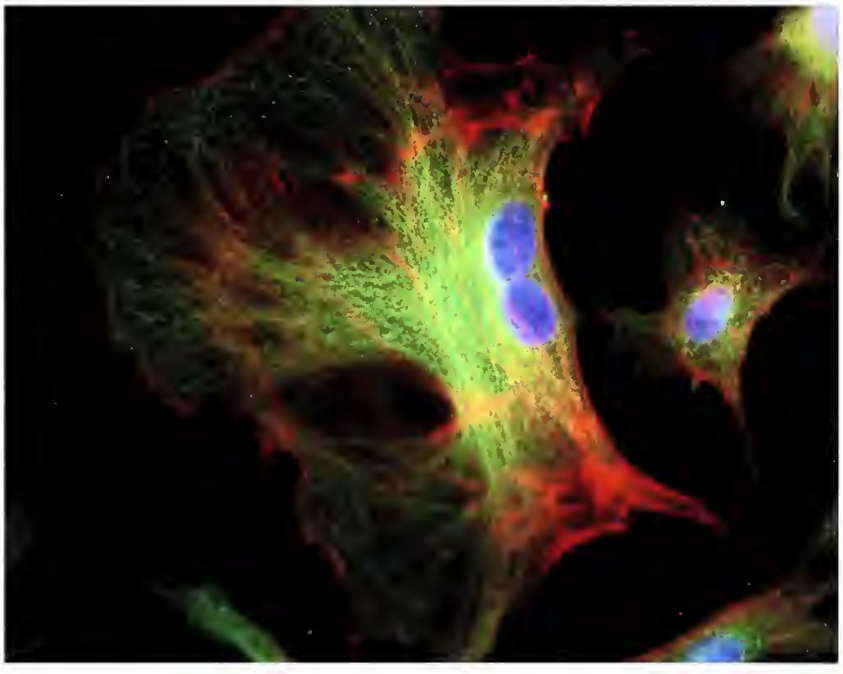

Figure 15: Immunocytochemistry of KRIT1 expression in BAE cells

KRIT1 staining localizes to the cytoplasm of BAE cells in a pattern suggesting an association with the cytoskeleton. (green = KRIT1; red = actin; blue = dapi)

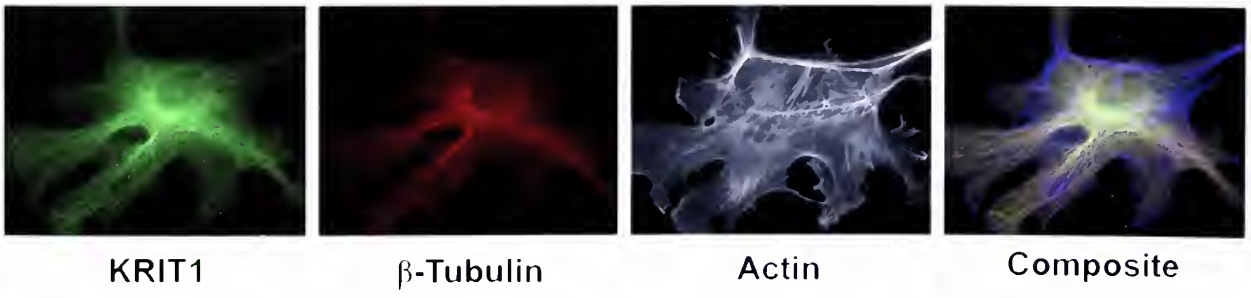

Figure 16: KRIT1 co-localizes with beta-tubulin

BAE cells were stained with antibodies to KRIT1, actin and beta-tubulin. KRIT1 staining reveals a filamentous pattern that differs from actin staining but overlaps with that of beta-tubulin; magnification 63X.

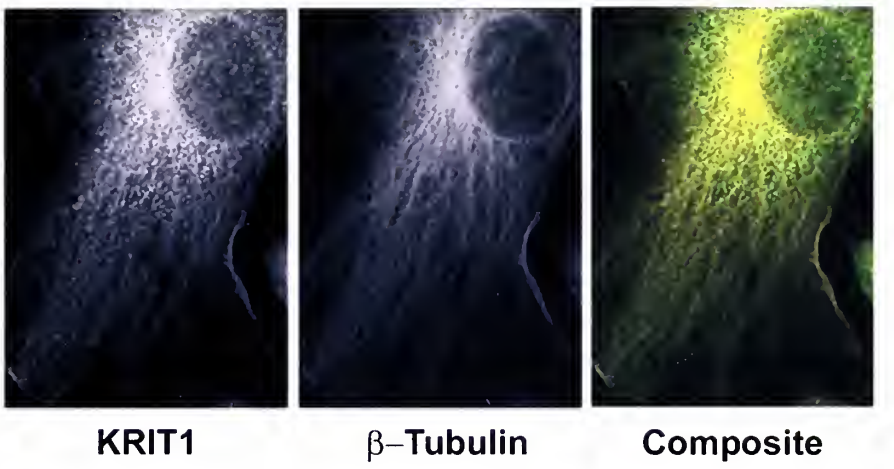

Figure 17: Confocal microscopy of BAE cell stained for beta-tubulin and KRIT1

Confocal image demonstrates co-localization of KRIT1 with beta-tubulin in a granular pattern along the length of microtubules; magnification 63X. KRIT1 staining was competed by the immunizing peptide (data not shown).

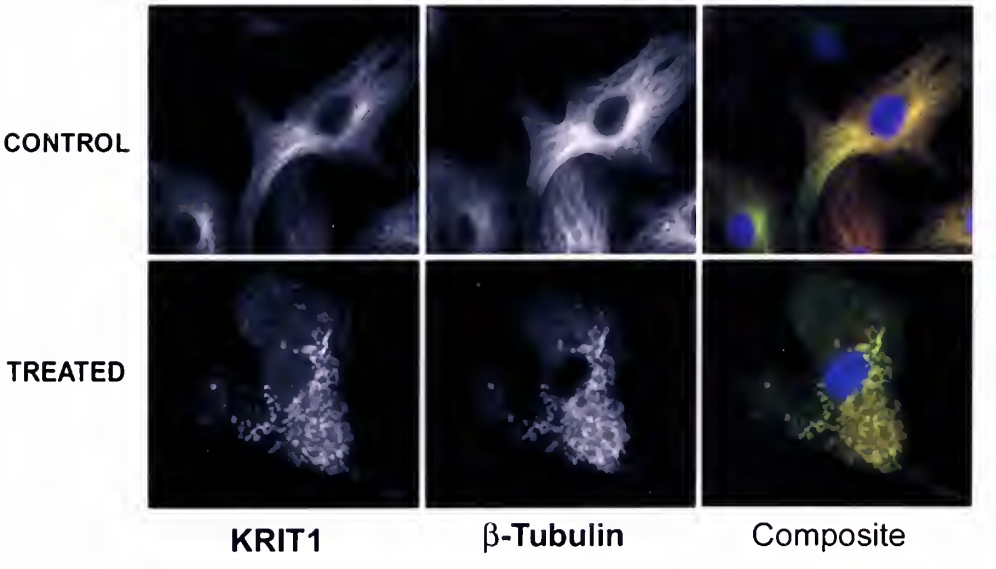

Figure 18: Immunocytochemistry of nocodazole treated BAE cells

Cultured endothelial cells were treated with nocodazole. Following treatment, KRIT1 staining changes to a pattern of cytoplasmic granules. KRIT1 continues to co-localize with beta-tubulin. (magnification 63x) (Composite image: green = KRIT1, red = beta-tubulin, blue = DAPI)

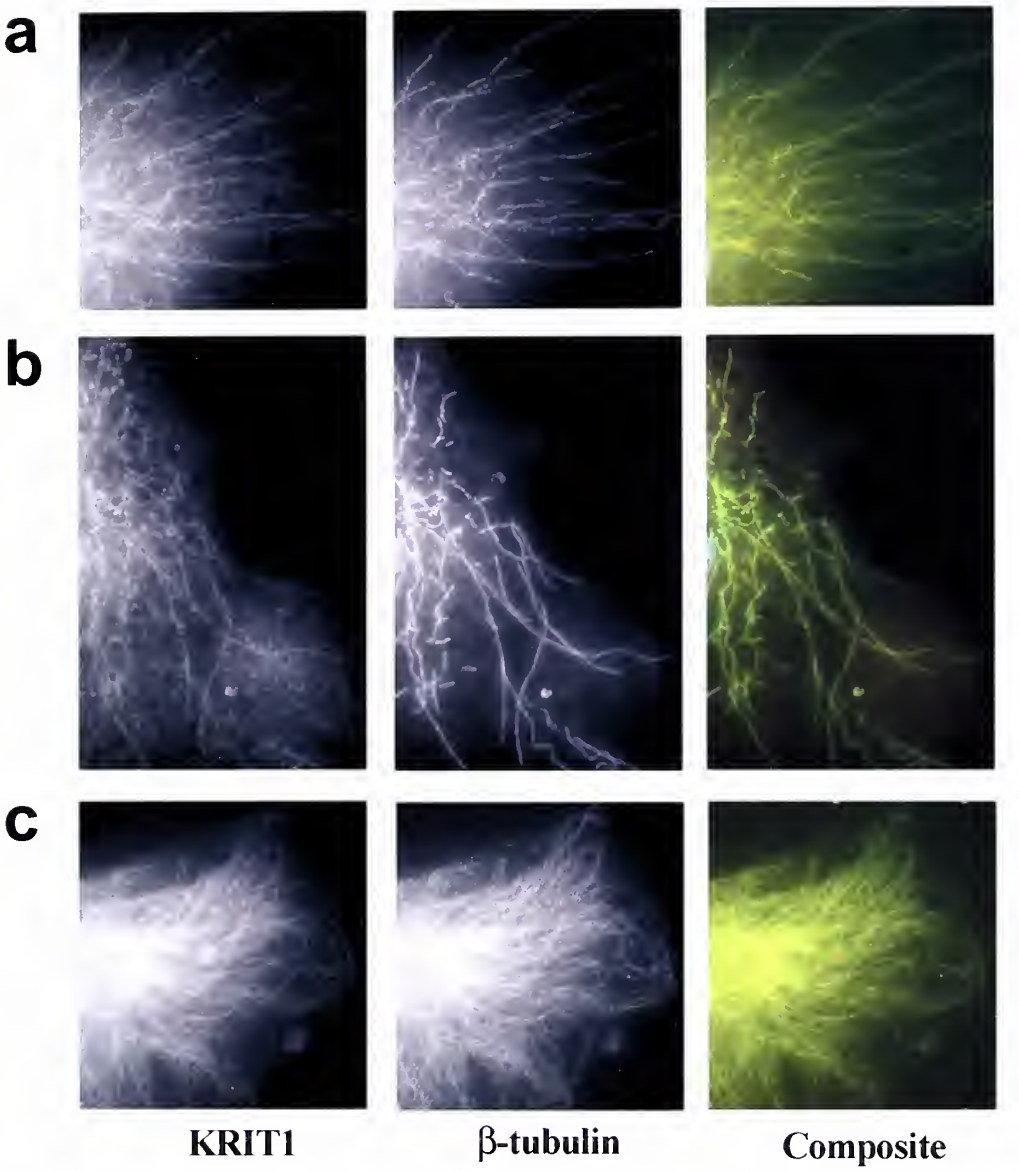

Figure 19: Co-localization of KRIT1 and beta-tubulin following cold treatment

Following indicated treatments of cultured BAECs, cells were stained for KRIT1 and beta-tubulin. Following 5 minutes (a) or 20 minutes (b) on ice, disruption of microtubules is observed, affecting both beta-tubulin and KRIT1 staining. Following 20 minutes of recovery at 37 ^{O}C, microtubules have repolymerized and KRIT1 staining is seen along their length (c).

KRIT1 interacts with tubulin

In order to determine whether KRIT1 and β-tubulin can be found together in a physical complex *in vivo*, co-immunoprecipitation experiments were performed. Either KRIT1 or β-tubulin antibody was used for immunoprecipitation from BAE cell lysates; the precipitated protein was evaluated by Western blotting using these same antibodies. Complexes immunoprecipitated with β-tubulin antibodies contain KRIT1 (Fig. 20a). Conversely, complexes immunoprecipitated with antibodies to KRIT1 contain β-tubulin (Fig. 20b). In contrast, control antibodies directed against proteins not believed to form a complex with either KRIT1 or β-tubulin are not found in these complexes (Fig. 20).

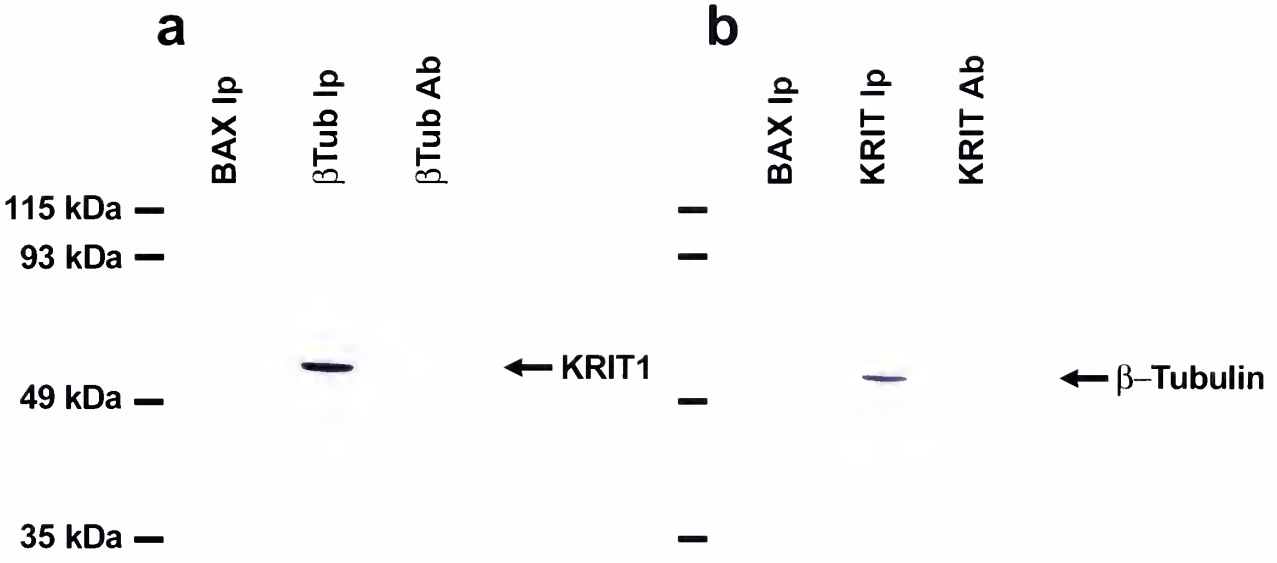

Figure 20: Co-immunoprecipitation of KRIT1 and beta-tubulin

BAE cell lysates were immunoprecipitated with mouse anti-Bax (lane 1), or mouse anti-beta-tubulin (lane 2). Lane 3 has been loaded with an equal amount of beta-tubulin antibody as lane 2 but without cell lysate. Western blots were prepared and probed with rabbit anti-KRIT1 antibody. The results demonstrate a band the size of KRIT1 only when lysate is precipitated with anti-beta-tubulin. (b) BAE cell lysates were immunoprecipitated with rabbit anti-Bax in lane 1 and rabbit anti-KRIT1 in lane 2. An equal amount of KRIT1 antibody has been loaded in lane 3. Western blots were prepared and probed with mouse antibody to beta-tubulin. The results demonstrate a band the size of beta-tubulin only when the lysate is precipitated with KRIT1.

Distribution of KRIT1 during endothelial cell mitosis

To further explore the association of KRIT1 with microtubules, we investigated endothelial cells throughout mitosis. During metaphase, KRIT1 staining was most intense at the spindle pole bodies and the plus ends of the astral microtubules at the kinetochore of the mitotic spindle, paralleling the location of β-tubulin (Figs. 21 & 22). Similarly, during anaphase A, when chromosomes are separated by shrinking of kinetochore fibers, the region of the overlapping plus ends of the interpolar microtubules of the interzone showed strong KRIT1 staining (Figs. 21 & 22), again consistent with plus end association. Finally, the staining pattern was particularly striking in late telophase during which KRIT1 localization is prominent at the midbody remnant, the site of cytokinesis where the extreme plus ends of microtubules of the two dividing cells overlap (Figs. 21 & 22). At these locations, KRIT1 staining can be seen to extend beyond the tip of β-tubulin expression (Fig. 22). This is consistent with KRIT1's location at the extreme plus end of microtubules.

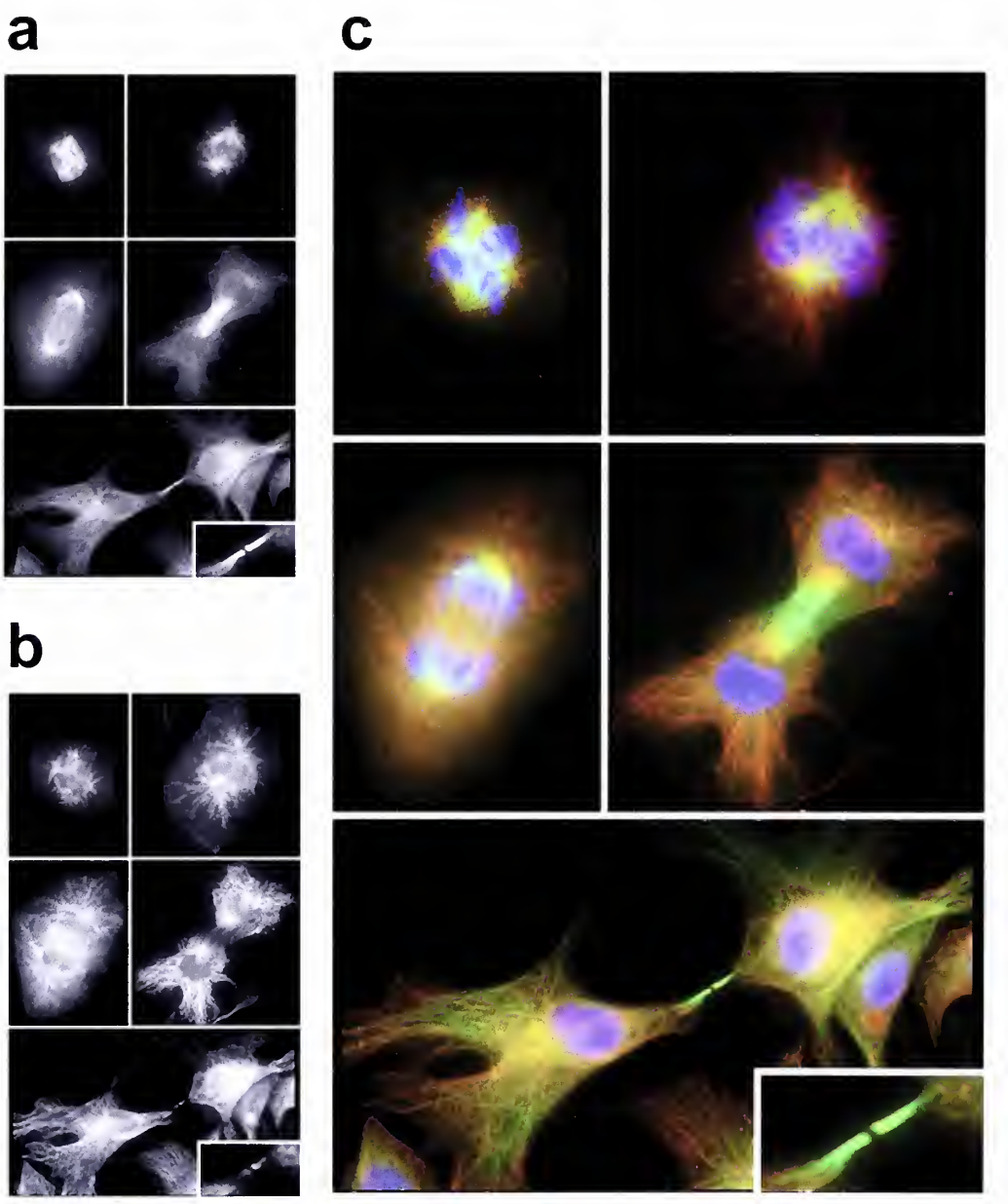

Figure 21: Mitotic BAE cells stained for KRIT1 and alpha-tubulin

Cultured endothelial cells were stained with antibodies to KRIT1 (green, (a)), DAPI (blue), and antibodies to alpha-tubulin (red, (b)). During prometaphase and metaphase, antibodies to KRIT1 intensely stain the spindle pole bodies and the mitotic spindle. As cells progress through anaphase and into telophase, KRIT1 staining is most striking in the central portion of the midbody. In late telophase KRIT1 localizes to the midbody remnant, consistent with the presence of KRIT1 at microtubule plus ends.

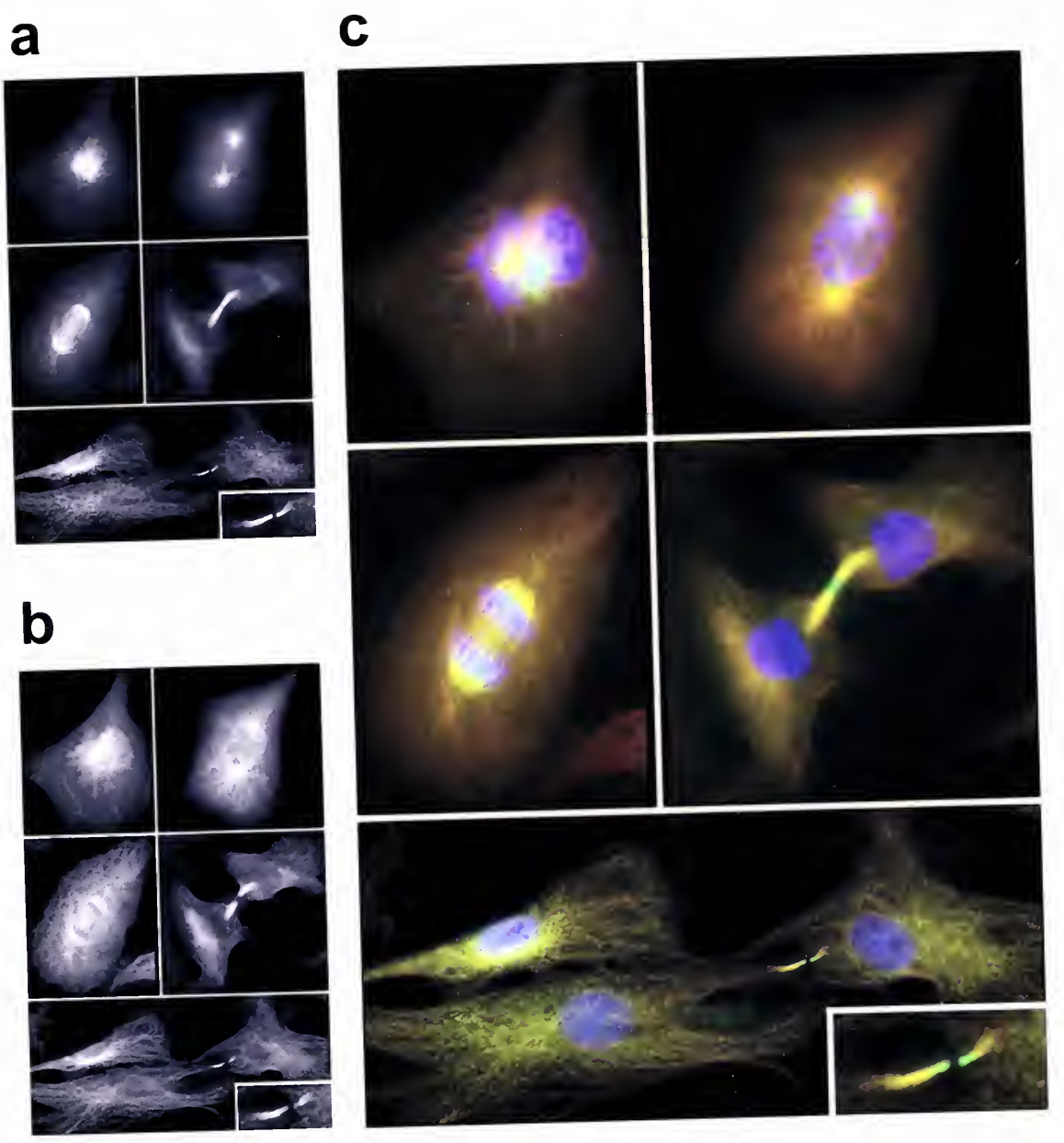

Figure 22: Mitotie BAE eells stained for KRIT1 and beta-tubulin

Cultured endothelial eells were stained with antibodies to KRIT1 (green, (a)), DAPI (blue), and antibodies to beta-tubulin (red, (b)). During prometaphase and metaphase, antibodies to KRIT1 intensely stain the spindle pole bodies and the mitotie spindle. As eells progress through anaphase and into telophase, KRIT1 staining is most striking in the central portion of the midbody. In late telophase KRIT1 loealizes to the midbody remnant, extending beyond beta-tubulin staining, eonsistent with the presenee of KRIT1 at mierotubule plus ends.

DISCUSSION

Despite the existence of KRIT1 in most human organs, the protein is not uniformly distributed, but instead specifically localizes to extracerebral and cerebral vascular endothelium, astrocytes, and pyramidal cells of the cerebral cortex. In a diverse array of tissues, antibodies to KRIT1 predominantly detect the protein in endothelial cells of capillaries and arterioles.

In the cerebral vasculature, KRIT1 is expressed by normal endothelial cells of capillaries, arterioles, and weakly by larger arteries. In addition, antibodies to this protein positively stain foot processes (endfeet) of astrocytes which abut the tunica adventitia of larger vessels on both the arterial and venous side of the circulation. The significance of this localization of KRIT1 is unclear; however, both of these structures – the endothelium and astrocytic endfeet – are important in the formation and maintenance of the brain-blood barrier. It is intriguing that in fenestrated capillaries of liver sinusoids, capillaries which lack tight junctions and whose endothelial cells fail to adhere to one another, KRIT1 is not expressed, and that cavernous malformation lesions predominantly develop in the unique environment established in the cerebral microvasculature.

The brain-blood barrier functions to protect the brain from fluctuations in plasma composition and from circulating agents which might disturb neural function. In addition, it assists in homeostatic regulation of the brain microenvironment necessary for normal function of the CNS (71). Cerebral capillaries are joined by a complex set of tight junctions (zonula occludens), which prevent transportation of hydrophilic substances to the brain parenchyma. Necessary polar substances, such as glucose, are

transported through specific carriers, such as GLUT-1 (72). This vascular-parenchymal interface is unique to the CNS, though a number of these properties are found to a lesser degree in peripheral capillary endothelium. Astrocytes and their foot processes, cells in which KRIT1 is expressed, contribute to the upregulation of endothelial tightening and downregulation of permeability factors which establishes and maintains the blood brain barrier (73-75).

Together these results confirm the presence of KRIT1 in the cerebral endothelial vasculature, and reveal that the protein is broadly, but specifically expressed by vascular endothelium in diverse human tissues. The presence of KRIT1 in extracerebral organs raises a central question: why are cavernous malformation lesions predominantly observed in the brain? Ultrastructural analysis of cavernous malformation lesions demonstrates an absence of tight junctions and astrocytic foot processes, indicating a role for blood-brain barrier breakdown in cerebral cavernous malformation pathophysiology (36). This data suggests that KRIT1 may participate in the development of the blood-brain barrier phenotype by assisting in focal adhesion of endothelial cells, or communication with astrocytes, or both. It is intriguing that the only other tissues in which cavernous malformation lesions are known to develop – the skin and retina –also contain elements of primitive neuroectoderm. An explanation for the focal nature of cavernous malformation lesions remains unclear, but perturbations of the blood brain barrier in cavernous malformation lesions and localization of the causative protein to these structures strongly suggests a specific role for KRIT1 in cerebral microvascular development.

These studies, in the context of known disease pathology, suggest that KRIT1 influences endothelial cells. Further studies, aimed at understanding this influence at the subcellular level, have identified an interaction between microtubules – highly dynamic structures important in determining cellular morphology – and KRIT1. The targeting and attachment of these polar structures appears to be directed by microtubule-associated proteins (MAPs). Microtubules are nucleated at minus ends originating at the centrosome/microtubule-organizing center; these minus ends are enriched in α-tubulin. Growth and shrinkage occurs at microtubule plus ends, which are enriched in β-tubulin; these plus ends explore the intracellular space and can be guided toward specialized membrane domains and chromosomes by specific plus-end-tracking proteins (76). We have shown that KRIT1 is a microtubule-associated protein that demonstrates increased localization to microtubule plus ends during mitosis. Immunoprecipitation experiments confirm that KRIT1 and β-tubulin are present within the same complexes, though they do not necessarily indicate a direct interaction.

The finding that KRIT1 can be located at microtubule plus ends suggests a potential role in targeting of microtubules, and the phenotype resulting from loss of KRIT1 function suggests a possible model for development of CCM lesions. One of the first stages of angiogenesis involves tube formation by endothelial cells; this tubulogenesis is triggered by interactions of endothelial cells with one another and with the extracellular matrix. Intercellular adhesion via PECAM1 (platelet endothelial cell adhesion molecule-1) provides signaling essential for endothelial tube formation (77, 78). It is intriguing that the GTPase activity of Krev1, an interacting partner of KRIT1 (58, 62, 79), is specifically activated by this interaction. This suggests a potential signaling

pathway connecting cell-cell contact via PECAM1 to the microtubule cytoskeleton via Krev1 and KRIT1. Such a connection involving Krev1 and the cytoskeleton has been made in yeast, in which the sole homologue of Krev1 is *Bud1/RSR1*, which is required for normal seleetion of the budding site, a process which involves targeting of microtubules (80). Similarly, ICAP1 α, the other known KRIT1- interacting protein, is known to bind to the cytoplasmie C-terminus of β1-integrin, thereby communicating information about cell-matrix interaetion to the cell interior. Consequently, the link between KRIT1 and microtubules, on the one hand, and KRIT1 with Krev1 and ICAP1 α on the other provides a potential pathway for signals from eell-cell contact and eell-matrix interaction, respeetively, to influence cytoskeletal structure (Fig. 23). The loss of this function could lead to the abnormal eapillary development seen in patients with CCM due to impaired microtubule targeting, resulting in impaired tubulogenesis.

This proposed function of KRIT1 in targeting microtubules in response to external signals is reminiscent of that of EB1, another plus end microtubule-binding protein. EB1 binds to the tumor suppressor APC, and it has been proposed that the activity of the Wnt signaling pathway is involved in the regulation of this interaction and the consequent targeting of microtubules (81).

These findings together provide the first localization of KRIT1 and also provide a framework for understanding the mechanism by which loss of KRIT1 causes human disease. Further work will be required to establish a role for KRIT1 in microtubule targeting and in determining the specific roles of other molecules involved in this pathway.

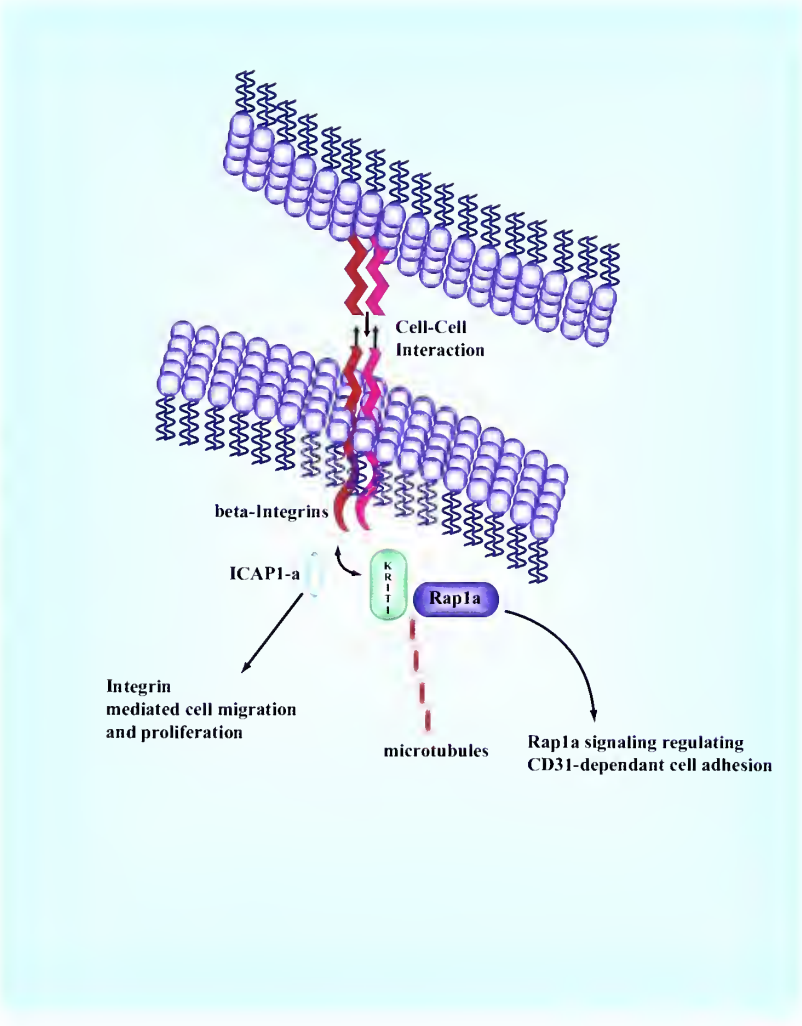

Figure 23: Proposed function for KRIT1 in the endothelial cell

CONCLUSIONS

This thesis has attempted to characterize the function of the cerebral cavernous malformation 1 protein, KRIT1, as a means to understanding hemorrhagic stroke and neurovascular development. Data uncovered here and elsewhere strongly suggest that KRIT1, a protein which is expressed in vascular endothelium of various organs, functions in communication between endothelial cell microtubules and the β-integrins, and is stimulated by and/or responds to cell-cell interactions. It is intriguing that when overexpressed, ICAP1 α disrupts focal adhesions in endothelial cells, perhaps simulating the cavernous malformation phenotype (82). It remains unclear to what degree KRIT1 participates in regulating ICAP1 α function and the development of focal adhesions, though both KRIT1 and the cytoplasmic β1 integrin tail compete for the same binding site on this protein (62, 79). Additionally, although KRIT1 is present in nearly all capillary beds, it fails to stain endothelial cells that lack tight junctions – hepatic sinusoids.

These discoveries have proceeded in a stepwise fashion in pursuit of examining the KRIT1 protein for the purpose of understanding cavernous malformation pathogenesis and cerebrovascular development. Given the disease phenotype, it seems likely that KRIT1 serves a unique purpose in the CNS. Further investigations will be aimed at further revealing this role, identifying *CCM2* and *CCM3*, and contextualizing these primary genetic determinants of stroke.

REFERENCES

1. Jafar JJ, Awad IA, Rosenwasser RH. Vascular malformations of the central nervous system. Philadelphia: Lippincott Williams & Wilkins, 1999:xvii, 540.
2. Barrow DL, Johnson DW. Historical Perspective and Classification of Spinal Vascular Malformations. In: Barrow DL, A. AI, eds. Spinal Vascular Malformations. Park Ridge: AANS, 1999:1-7.
3. Ojemann RG, Heros RC, Crowell RM. Surgical Management of Cerebrovascular Disease. Baltimore: Williams & Wilkins, 1988.
4. Masson C, Godefroy O, Leclerc X, Colombani JM, Leys D. Cerebral venous infarction following thrombosis of the draining vein of a venous angioma (developmental abnormality). Cerebrovasc Dis 2000; 10:235-8.
5. Guttmacher AE, Marchuk DA, White RI, Jr. Hereditary hemorrhagic telangiectasia. N Engl J Med 1995; 333:918-24.
6. Awad IA, Robinson JR, Jr., Mohanty S, Estes ML. Mixed vascular malformations of the brain: clinical and pathogenetic considerations. Neurosurgery 1993; 33:179-88; discussion 188.
7. Robinson JR, Awad IA, Little JR. Natural history of the cavernous angioma. J Neurosurg 1991; 75:709-14.
8. Kamiryo T, Nelson PK, Bose A, Zalzal P, Jafar JJ. Familial arteriovenous malformations in siblings. Surg Neurol 2000; 53:255-9.

9. Herzig R, Burval S, Vladyka V, et al. Familial occurrence of cerebral arteriovenous malformation in sisters: case report and review of the literature. Eur J Neurol 2000; 7:95-100.

10. Amin-Hanjani S, Robertson R, Arginteanu MS, Scott RM. Familial intracranial arteriovenous malformations. Case report and review of the literature. Pediatr Neurosurg 1998; 29:208-13.

11. Brilli RJ, Sacchetti A, Neff S. Familial arteriovenous malformations in children. Pediatr Emerg Care 1995; 11:376-8.

12. Goto S, Abe M, Tsuji T, Tabuchi K. Familial arteriovenous malformations of the brain--two case reports. Neurol Med Chir (Tokyo) 1994; 34:221-4.

13. Morita T, Iwai T, Takada M, et al. [Familial occurrence of intracranial arteriovenous malformation]. No Shinkei Geka 1985; 13:181-6.

14. Boyd MC, Steinbok P, Paty DW. Familial arteriovenous malformations. Report of four cases in one family. J Neurosurg 1985; 62:597-9.

15. Schievink WI. Genetics of intracranial aneurysms. Neurosurgery 1997; 40:651-62; discussion 662-3.

16. ter Berg HW, Dippel DW, Limburg M, Schievink WI, van Gijn J. Familial intracranial aneurysms. A review. Stroke 1992; 23:1024-30.

17. Jain KK. Familial intracranial aneurysms. Review of literature and presentation of six new cases. Acta Neurochir (Wien) 1974; 30:129-37.

18. Vikkula M, Boon LM, Carraway KL, et al. Vascular dysmorphogenesis caused by an activating mutation in the receptor tyrosine kinase TIE2. Cell 1996; 87:1181-90.

19. Heutink P, Haitjema T, Breedveld GJ, et al. Linkage of hereditary haemorrhagic telangiectasia to chromosome 9q34 and evidence for locus heterogeneity. J Med Genet 1994; 31:933-6.

20. McDonald MT, Papenberg KA, Ghosh S, et al. A disease locus for hereditary haemorrhagic telangiectasia maps to chromosome 9q33-34. Nat Genet 1994; 6:197-204.

21. Shovlin CL, Hughes JM, Tuddenham EG, et al. A gene for hereditary haemorrhagic telangiectasia maps to chromosome 9q3. Nat Genet 1994; 6:205-9.

22. Johnson DW, Berg JN, Gallione CJ, et al. A second locus for hereditary hemorrhagic telangiectasia maps to chromosome 12. Genome Res 1995; 5:21-8.

23. Vincent P, Plauchu H, Hazan J, Faure S, Weissenbach J, Godet J. A third locus for hereditary haemorrhagic telangiectasia maps to chromosome 12q [published erratum appears in Hum Mol Genet 1995 Jul;4(7):1243]. Hum Mol Genet 1995; 4:945-9.

24. Berg JN, Gallione CJ, Stenzel TT, et al. The activin receptor-like kinase 1 gene: genomic structure and mutations in hereditary hemorrhagic telangiectasia type 2. Am J Hum Genet 1997; 61:60-7.

25. Shovlin CL, Hughes JM, Scott J, Seidman CE, Seidman JG. Characterization of endoglin and identification of novel mutations in hereditary hemorrhagic telangiectasia. Am J Hum Genet 1997; 61:68-79.

26. Marchuk DA. Genetic abnormalities in hereditary hemorrhagic telangiectasia. Curr Opin Hematol 1998; 5:332-8.

27. Li DY, Sorensen LK, Brooke BS, et al. Defective angiogenesis in mice lacking endoglin. Science 1999; 284:1534-7.

28. Laberge-le Couteulx S, Jung HH, Labauge P, et al. Truncating mutations in CCM1, encoding KRIT1, cause hereditary cavernous angiomas. Nat Genet 1999; 23:189-93.

29. Sahoo T, Johnson EW, Thomas JW, et al. Mutations in the gene encoding KRIT1, a Krev-1/rap1a binding protein, cause cerebral cavernous malformations (CCM1). Hum Mol Genet 1999; 8:2325-33.

30. Robinson JR, Awad IA, Magdinec M, Paranandi L. Factors predisposing to clinical disability in patients with cavernous malformations of the brain. Neurosurgery 1993; 32:730-5; discussion 735-6.

31. Perl J, Ross, J. Diagnostic Imaging of Cavernous Malformations. In: Awad IA, Barrow, D., ed. Cavernous Malformations. Park Ridge: AANS, 1993:37-48.

32. Del Curling O, Kelly DL, Elster AD, Craven TE. An analysis of the natural history of cavernous angiomas. J Neurosurg 1991; 75:702-8.

33. Sage MR, Brophy, B.P., Sweeney, C., Phipps, S., Perrerr, L.V., Sandhu, A., Albertyn, L.E. Cavernous haemangiomas (angiomas) of the brain: clinically significant lesions. Australasian Radiology. 1993; 37:147-155.

34. Otten P, Pizzolato, G.P., Rilliet, B., Berney, J. 131 cases of cavernous angioma (cavernomas) of the CNS, discovered by retrospective analysis of 24,535 autopsies. Neurochirurgie 1989; 35:82-83.

35. Zyed A, Hayman LA, Bryan RN. MR imaging of intracerebral blood: diversity in the temporal pattern at 0.5 and 1.0 T. AJNR Am J Neuroradiol 1991; 12:469-74.

36. Clatterbuck RE, Eberhart CG, Crain BJ, Rigamonti D. Ultrastructural and immunocytochemical evidence that an incompetent blood-brain barrier is related to the pathophysiology of cavernous malformations. J Neurol Neurosurg Psychiatry 2001; 71:188-92.

37. Wong JH, Awad IA, Kim JH. Ultrastructural pathological features of cerebrovascular malformations: a preliminary report. Neurosurgery 2000; 46:1454-9.

38. Russell DS, Rubenstein, L.J. Pathology of Tumors of the Nervous system. Baltimore: Williams and Wilkins, 1989:730-736.

39. Clatterbuck RE, Rigamonti D. Cherry angiomas associated with familial cerebral cavernous malformations. Case illustration. J Neurosurg 2002; 96:964.

40. Barrow D, Krisht, A. Cavernous malformations and hemorrhage. In: Awad IA BD, ed. Cavernous Malformations. Park Ridge: AANS, 1993:65-80.

41. Michael JC, Levin PM. Multiple telangiectases of brain: a discussion of hereditary factors in their development. Arch. Neurol. Psychiat. 1936; 36:514-536.

42. Kidd HA, Cumings JN. Cerebral angiomata in an Icelandic family. Lancet 1947; I:747-748.

43. Hayman LA, Evans RA, Ferrell RE, Fahr LM, Ostrow P, Riccardi VM. Familial cavernous angiomas: natural history and genetic study over a 5- year period. Am J Med Genet 1982; 11:147-60.

44. Gunel M, Awad IA, Anson J, Lifton RP. Mapping a gene causing cerebral cavernous malformation to 7q11.2-q21. Proc Natl Acad Sci U S A 1995; 92:6620-4.

45. Dubovsky J, Zabramski JM, Kurth J, et al. A gene responsible for cavernous malformations of the brain maps to chromosome 7q. Hum Mol Genet 1995; 4:453-8.

46. Gunel M, Awad IA, Finberg K, et al. A founder mutation as a cause of cerebral cavernous malformation in Hispanic Americans. N Engl J Med 1996; 334:946-51.

47. Craig HD, Gunel M, Cepeda O, et al. Multilocus linkage identifies two new loci for a mendelian form of stroke, cerebral cavernous malformation, at 7p15-13 and 3q25.2-27. Hum Mol Genet 1998; 7:1851-8.

48. Johnson EW, Iyer LM, Rich SS, et al. Refined localization of the cerebral cavernous malformation gene (CCM1) to a 4-cM interval of chromosome 7q contained in a well-defined YAC contig. Genome Res 1995; 5:368-80.

49. Chen DH, Lipe HP, Qin Z, Bird TD. Cerebral cavernous malformation: novel mutation in a Chinese family and evidence for heterogeneity. J Neurol Sci 2002; 196:91-6.

50. Couteulx SL, Brezin AP, Fontaine B, Tournier-Lasserve E, Labauge P. A novel KRIT1/CCM1 truncating mutation in a patient with cerebral and retinal cavernous angiomas. Arch Ophthalmol 2002; 120:217-8.

51. Davenport WJ, Siegel AM, Dichgans J, et al. CCM1 gene mutations in families segregating cerebral cavernous malformations. Neurology 2001; 56:540-543.

52. Lucas M, Solano F, Zayas MD, et al. Spanish families with cerebral cavernous angioma do not bear 742C-->T Hispanic American mutation of the KRIT1 gene. Ann Neurol 2000; 47:836.

53. Verlaan DJ, Davenport WJ, Stefan H, Sure U, Siegel AM, Rouleau GA. Cerebral cavernous malformations: mutations in Krit1. Neurology 2002; 58:853-7.

54. Verlaan DJ, Siegel AM, Rouleau GA. Krit1 missense mutations lead to splicing errors in cerebral cavernous malformation. Am J Hum Genet 2002; 70:1564-7.

55. Zhang J, Clatterbuck RE, Rigamonti D, Dietz HC. Mutations in KRIT1 in familial cerebral cavernous malformations. Neurosurgery 2000; 46:1272-7; discussion 1277-9.

56. Cave-Riant F, Denier C, Labauge P, et al. Spectrum and expression analysis of KRIT1 mutations in 121 consecutive and unrelated patients with Cerebral Cavernous Malformations. Eur J Hum Genet 2002; 10:733-40.

57. Laurans MSH, DiLuna ML, Shin D, et al. Mutational analysis of 206 cavernous malformation families. (submitted to) Journal of Neurosurgery 2003.

58. Serebriiskii I, Estojak J, Sonoda G, Testa JR, Golemis EA. Association of Krev-1/rap1a with Krit1, a novel ankyrin repeat- containing protein encoded by a gene mapping to 7q21-22. Oncogene 1997; 15:1043-9.

59. Leach SD, Berger DH, Davidson BS, Curley SA, Tainsky MA. Enhanced Krev-1 expression inhibits the growth of pancreatic adenocarcinoma cells. Pancreas 1998; 16:491-8.

60. Eerola I, McIntyre B, Vikkula M. Identification of eight novel 5'-exons in cerebral capillary malformation gene-1 (CCM1) encoding KRIT1. Biochim Biophys Acta 2001; 1517:464-7.

61. Sahoo T, Goenaga-Diaz E, Serebriiskii IG, et al. Computational and Experimental Analyses Reveal Previously Undetected Coding Exons of the KRIT1 (CCM1) Gene. Genomics 2001; 71:123-126.

62. Zhang J, Clatterbuck RE, Rigamonti D, Chang DD, Dietz HC. Interaction between krit1 and icap1alpha infers perturbation of integrin beta1-mediated angiogenesis in the pathogenesis of cerebral cavernous malformation. Hum Mol Genet 2001; 10:2953-60.

63. Thompson DW, Furlan AJ. Clinical epidemiology of stroke. Neurol Clin 1996; 14:309-15.

64. Kiely DK, Wolf PA, Cupples LA, Beiser AS, Myers RH. Familial aggregation of stroke. The Framingham Study. Stroke 1993; 24:1366-71.

65. Brass LM, Isaacsohn JL, Merikangas KR, Robinette CD. A study of twins and stroke. Stroke 1992; 23:221-3.

66. Joutel A, Corpechot C, Ducros A, et al. Notch3 mutations in CADASIL, a hereditary adult-onset condition causing stroke and dementia. Nature 1996; 383:707-10.

67. Goto Y, Nonaka I, Horai S. A mutation in the tRNA(Leu)(UUR) gene associated with the MELAS subgroup of mitochondrial encephalomyopathies. Nature 1990; 348:651-3.

68. Clatterbuck RE, Cohen B, Gailloud P, Murphy K, Rigamonti D. Vertebral hemangiomas associated with familial cerebral cavernous malformation: segmental disease expression. Case report. J Neurosurg 2002; 97:227-30.

69. Roda A, Pasini P, Guardigli M, Baraldini M, Musiani M, Mirasoli M. Bio- and chemiluminescence in bioanalysis. Fresenius J Anal Chem 2000; 366:752-9.

70. De Brabander M, De May J, Joniau M, Geuens G. Ultrastructural immunocytochemical distribution of tubulin in cultured cells treated with microtubule inhibitors. Cell Biol Int Rep 1977; 1:177-83.

71. Abbott NJ. Astrocyte-endothelial interactions and blood-brain barrier permeability. J Anat 2002; 200:629-38.

72. Pardridge WM, Boado RJ, Farrell CR. Brain-type glucose transporter (GLUT-1) is selectively localized to the blood-brain barrier. Studies with quantitative western blotting and in situ hybridization. J Biol Chem 1990; 265:18035-40.

73. Schwaninger M, Sallmann S, Petersen N, et al. Bradykinin induces interleukin-6 expression in astrocytes through activation of nuclear factor-kappaB. J Neurochem 1999; 73:1461-6.

74. Bauer HC, Bauer H. Neural induction of the blood-brain barrier: still an enigma. Cell Mol Neurobiol 2000; 20:13-28.

75. Gloor SM, Weber A, Adachi N, Frei K. Interleukin-1 modulates protein tyrosine phosphatase activity and permeability of brain endothelial cells. Biochem Biophys Res Commun 1997; 239:804-9.

76. Schuyler SC, Pellman D. Microtubule "plus-end-tracking proteins": The end is just the beginning. Cell 2001; 105:421-4.

77. Albelda SM, Muller WA, Buck CA, Newman PJ. Molecular and cellular properties of PECAM-1 (endoCAM/CD31): a novel vascular cell-cell adhesion molecule. J Cell Biol 1991; 114:1059-68.

78. Reedquist KA, Ross E, Koop EA, et al. The small GTPase, Rap1, mediates CD31-induced integrin adhesion. J Cell Biol 2000; 148:1151-8.

79. Zawistowski JS, Serebriiskii IG, Lee MF, Golemis EA, Marchuk DA. KRIT1 association with the integrin-binding protein ICAP-1: a new direction in the elucidation of cerebral cavernous malformations (CCM1) pathogenesis. Hum Mol Genet 2002; 11:389-96.

80. Ruggieri R, Bender A, Matsui Y, et al. RSR1, a ras-like gene homologous to Krev-1 (smg21A/rap1A): role in the development of cell polarity and interactions with the Ras pathway in Saccharomyces cerevisiae. Mol Cell Biol 1992; 12:758-66.

81. Juwana JP, Henderikx P, Mischo A, et al. EB/RP gene family encodes tubulin binding proteins. Int J Cancer 1999; 81:275-84.

82. Bouvard D, Vignoud L, Dupe-Manet S, et al. Disruption of Focal Adhesions by Integrin Cytoplasmic Domain-associated Protein-1alpha. J Biol Chem 2003; 278:6567-6574.

HARVEY CUSHING/JOHN HAY WHITNEY MEDICAL LIBRARY

MANUSCRIPT THESES

Unpublished theses submitted for the Master's and Doctor's degrees and deposited in the Medical Library are to be used only with due regard to the rights of the authors. Bibliographical references may be noted, but passages must not be copied without permission of the authors, and without proper credit being given in subsequent written or published work.

This thesis by
has been used by the following person, whose signatures attest their acceptance of the above restrictions.

NAME AND ADDRESS **DATE**